

Review

Recent advances in innovative strategies for enhanced cancer photodynamic therapy

Tingting Hu¹, Zhengdi Wang¹, Weicheng Shen¹, Ruizheng Liang¹✉, Dan Yan²✉ and Min Wei¹✉

1. State Key Laboratory of Chemical Resource Engineering, Beijing Advanced Innovation Center for Soft Matter Science and Engineering, Beijing University of Chemical Technology, Beijing 100029, P. R. China.
2. Beijing Friendship Hospital, Capital Medical University, Beijing 100050, P. R. China.

✉ Corresponding author: E-mail: weimin@mail.buct.edu.cn (Min Wei); danyan@ccmu.edu.cn (Dan Yan); liangrz@mail.buct.edu.cn (Ruizheng Liang).

© The author(s). This is an open access article distributed under the terms of the Creative Commons Attribution License (<https://creativecommons.org/licenses/by/4.0/>). See <http://ivyspring.com/terms> for full terms and conditions.

Received: 2020.10.08; Accepted: 2020.12.05; Published: 2021.01.15

Abstract

Photodynamic therapy (PDT), a non-invasive therapeutic modality, has received increasing attention owing to its high selectivity and limited side effects. Although significant clinical research progress has been made in PDT, the breadth and depth of its clinical application have not been fully realized due to the limitations such as inadequate light penetration depth, non-targeting photosensitizers (PSs), and tumor hypoxia. Consequently, numerous investigations put their emphasis on innovative strategies to overcome the aforementioned limitations and enhance the therapeutic effect of PDT. Herein, up-to-date advances in these innovative methods for PDT are summarized by introducing the design of PS systems, their working mechanisms and application examples. In addition, current challenges of these innovative strategies for clinical application, and future perspectives on further improvement of PDT are also discussed.

Key words: photodynamic therapy, light source, photosensitizers, tumor hypoxia

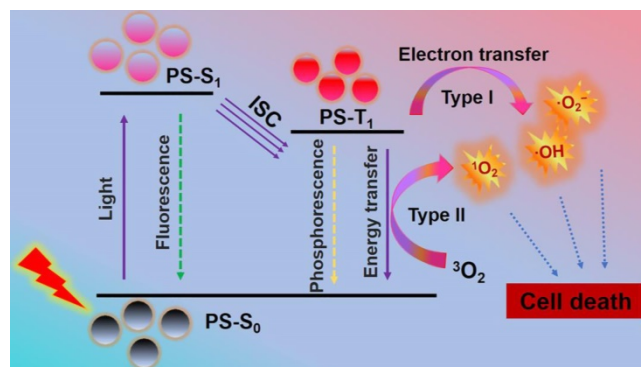
Introduction

As a global medical problem in modern society, cancer is a serious threat to human health due to its high morbidity and mortality [1,2]. Therefore, novel cancer therapies with few side effects and excellent curative effects are highly needed. Photodynamic therapy (PDT), a cancer therapy with clinical appeal, has received extensive attention owing to its high selectivity, minimally invasive nature, and limited side effects [3,4]. Briefly, PDT adopts light-excited photosensitizers (PSs) to generate lethal reactive oxygen species (ROS), such as singlet oxygen ($^1\text{O}_2$), superoxide radicals (O_2^-) and hydroxyl radicals ($\cdot\text{OH}$). It works mainly through type I and type II mechanism (**Scheme 1**). Initially, PSs in ground state (S_0) can transform into excited singlet state (S_1 or $^1\text{PS}^*$) by absorbing light. Then, the $^1\text{PS}^*$ can change to triplet state (T_1 or $^3\text{PS}^*$) through intersystem crossing (ISC) [30]. In type II mechanism, the PDT effect is highly dependent on the oxygen (O_2) content, since there is direct energy transfer from $^3\text{PS}^*$ to surrounding O_2 to produce highly reactive $^1\text{O}_2$ [5-7]. While in type I mechanism, the $^3\text{PS}^*$ usually undergo electron

transfer with cellular substrates in a physiological environment to produce toxic free radicals (e.g. $\cdot\text{OH}$ and O_2^-) without O_2 dependence. The resultant ROS can cause irreversible and permanent damage to cancer cells, and eventually lead to cell apoptosis and/or apoptosis, immune response, and microvascular damage [8-10].

Generally, light source, PSs and O_2 are the three necessary components of PDT. With the continuous development of PSs and optical fiber-guided laser transmission systems, PDT has evolved from theoretical research to clinical research and expanded to imaging and treatment of various cancer and non-cancer diseases [11-15]. However, like other therapies, the breadth and depth of PDT's efficacy have not been fully realized due to the limitations such as light penetration depth, inefficient PSs, targeted distribution, and tumor hypoxia [16-20]. As PDT works only when the light reaches the target area, its therapeutic effect is quite limited to cancers in the skin areas or areas adjacent to the organ. In term of PSs, the difficulty of systemic administration is that

PSs are generally easy to aggregate and lack targeting, thus limiting the clinical PDT efficacy. In addition, due to the excessive proliferation of cancer cells and insufficient blood supply in tumors, the O_2 content in tumors is severely insufficient, resulting in a significant reduction of PDT efficacy. As a result, extensive research is being carried out to optimize viable PSs systems to overcome the aforementioned limitations.



Scheme 1. Mechanism of photodynamic reaction: PSs in S_0 can transform into S_1 by absorbing light. The S_1 can change to T_1 through ISC. The direct energy transfer from T_1 to 3O_2 or electron transfer between T_1 and cellular substrates can produce ROS to induce cell death. Abbreviations: S_0 : ground state; S_1 : excited singlet state; T_1 : triplet state.

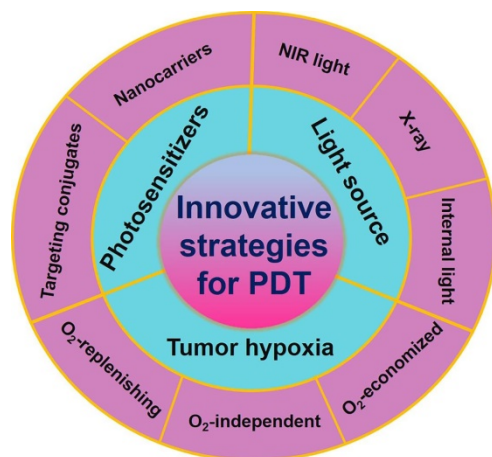


Figure 1. Schematic illustration of the innovative strategies for overcoming limitations (such as inadequate light penetration depth, non-targeting PSs, and tumor hypoxia) and enhancing the therapeutic effect of PDT. Abbreviations: PDT: photodynamic therapy.

Great efforts have been devoted to developing PDT and a number of strategies have been rationally proposed in recent years. Advances in PDT have been discussed a lot in previous reviews, and some of them emphasize on specific aspects, such as hypoxic tumor, tumor microenvironment (TME)-responsive PDT, types of PSs and their activation strategies, and the nanomaterials used in PDT. New techniques applied in PDT, such as ultrasound, microwaves and X-rays have also been reviewed [30,142-145]. Nevertheless, little attention has been paid to the comprehensive and in-depth profile of recent strategies in PDT. In this

review, we summarize and discuss the latest advancements and paradigms of PDT in cancer therapy by introducing the design of PS systems, their working mechanisms and application examples with a focus on the innovative strategies to improve the light penetration depth, ROS production efficiency, stability and targeted ability of PSs, and tumor hypoxia (Figure 1). At the end of the review, upcoming challenges and future perspectives of these innovative strategies (especially in clinical application) are discussed.

Light Source

For PDT in cancer treatment, appropriate light source, adequate PSs, and abundant O_2 are the three essential components required in tumor tissues [21,22]. Among them, the choice of light source is particularly important because the light needs to be delivered homogeneously to the target area to ensure the therapeutic effect. Most PSs used for PDT have maximum absorption in the visible region (400–700 nm). To date, four types of laser light sources (argon-pumped lasers, metal-vapor-pumped lasers (Au- or Cu-vapor lasers), solid-state lasers (Nd:YAG lasers, Ho:YAG lasers, KTP:YAG/dye lasers), and diode lasers) and three non-laser light sources (lamp light, light-emitting diodes (LEDs), and daylight) have been tested in PDT [23-28]. Some of them have been used clinically, such as a red light argon dye laser, Nd:YAG laser, a red light (635 nm) LED lamp, a 570–670 nm wavelength red light lamp, green light (520 nm), 420-nm blue light-emitting diode, daylight, etc. However, the penetration depth of these light sources is quite low (1–6 mm) for two reasons: (1) many endogenous chromophores in biological tissues, such as cytochromes and haemoglobin, can absorb visible light; (2) the heterogeneous structure of biological tissues can lead to light scattering, diffusing and disorienting, and thus significantly affects the photodynamic effect [30]. As a result, near-infrared (NIR) light, X-ray, interstitial light, and internal light are employed in innovative strategies for deeper penetration depth [20,29]. On this basis, recent research progress of PDT in light source will be discussed in detail in this section.

NIR light

It is generally known that NIR light (700–1350 nm), which can be divided into NIR I (700–1000 nm) region and NIR II (1000–1350 nm) region, is the ‘optical window’ of biological tissues. Compared with visible light, long-wavelength NIR light minimizes the degree of tissue scattering with a penetration depth exceeding 1 cm. The utilization of NIR light not only allows deeper tumor penetration but also

reduces the phototoxicity on healthy tissues [20]. Recently, in the work of Liu *et al.* [31], a NIR light-activated PDT nanosystem based on the combination of porphyrinic metal-organic frameworks (MOFs) and upconversion nanoparticles (UCNPs) was reported. The system was synthesized by growing porphyrinic MOFs on Nd^{3+} -sensitized UCNPs to achieve Janus nanostructures. UCNPs could convert the low-energy NIR light to high-energy UV or visible light so as to excite porphyrinic MOFs to generate ROS. *In vitro* and *in vivo* tests certified the superior therapeutic effect of NIR-activated PDT. In another work, Zhang *et al.* [32] proposed a similar strategy that integrated rare-earth-doped UCNPs with graphene quantum dot (GQD) to form GQD-decorated UCNPs (UCNPs-GQD). Under NIR excitation, UCNPs could emit UV-vis light to excite the prominent $^1\text{O}_2$ generation of GQD for highly efficacious PDT (Figure 2A). This

upconversion technique seems quite promising in increasing penetration depth, however, it is limited by low energy conversion efficiency to a certain extent.

A recent breakthrough reported by Gao *et al.* [33] in NIR-activated PDT solved the above problem, and high-efficiency NIR-activated PSs were developed. This work assembled isophthalic acid (IPA, a type of room-temperature phosphorescence (RTP) compound) into the layered double hydroxides (LDHs) interlayer gallery, which formed an IPA/LDH nano hybrid (Figure 2B). In this PS system, the LDH monolayers provided space- and interface-confined microenvironments for IPA, facilitating the two-photon-induced generation of long-lived triplet exciton with a $^1\text{O}_2$ quantum yield up to 0.74. Due to the excellent tissue penetration ability of 808 nm light, the IPA/LDH nano hybrid displayed superior anticancer performance with extremely low toxicity.

This work provides a proof of concept that long-lived RTP compounds can be used as two-photon-activated PSs for NIR-activated PDT.

X-ray

In spite of the popularity of NIR light, its application is still limited by the penetration depth (10–15 mm). As a kind of ionizing radiation source, X-ray has been widely applied in clinical tumor imaging and therapy owing to its unrestricted penetration depth in human body [29]. With the above advantage, X-ray can be adopted as a light source to excite PSs. The X-ray-induced PDT (X-PDT) can be categorized as: (1) metal-based X-PDT; (2) rare-earth-element-based X-PDT; (3) quantum dot (QD)-based X-PDT; (4) silicon-based X-PDT [52]. For example, Sun *et al.* [34] designed a new PS system (R-AIE-Au) based on rose bengal (RB)-conjugated aggregation-

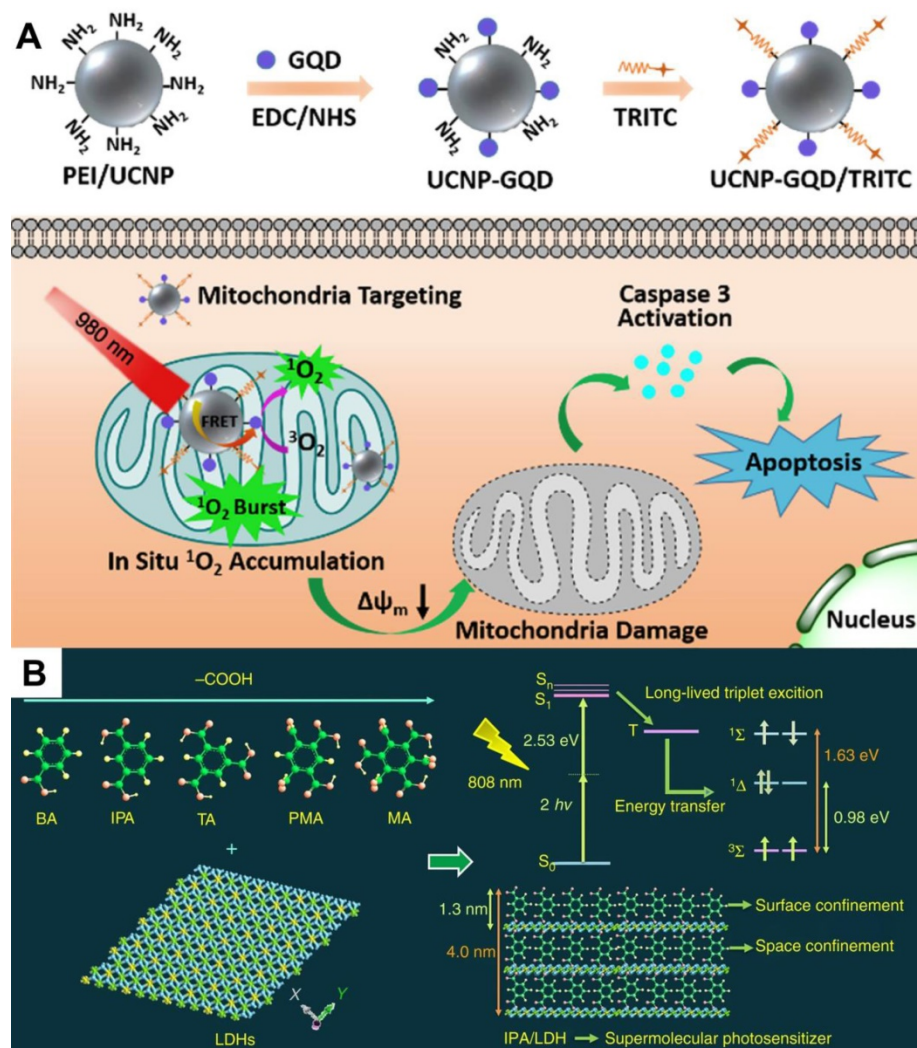


Figure 2. (A) Schematic diagram of UCNPs-GQD with mitochondria-targeting potency for high-efficient cells apoptosis upon laser irradiation. Reproduced with permission from Ref. [32], Copyright © 2017, Elsevier. (B) Schematic illustration of IPA/LDH nano hybrids as two-photon PSs for $^1\text{O}_2$ generation under 808 nm NIR laser. Reproduced with permission from Ref. [33], Copyright © 2018, Nature Publishing Group. Abbreviations: UCNPs: upconversion nanoparticles; GQD: graphene quantum dot; IPA: isophthalic acid; LDH: layered double hydroxides; PSs: photosensitizers; $^1\text{O}_2$: singlet oxygen; NIR: near-infrared.

induced emission gold clustoluminogens (AIE-Au) for low-dose metal-based X-PDT. Under X-ray irradiation, the Au atoms efficiently converted X-ray to luminescence and further excited conjugated RB for PDT (**Figure 3A**). *In vitro* and *in vivo* studies verified that R-AIE-Au could generate X-ray-triggered ROS through the unique X-PDT mechanism, thereby realizing the effective treatment of radioresistant cancers. This new PS system possesses the potential for the treatment of deep penetrating tumors. In another study, cerium (Ce)-doped highly fluorescent NaCeF₄:Gd,Tb scintillating nanoparticles (ScNPs) for rare-earth-element-based X-PDT were reported by Zhong *et al.* [35]. The Ce and Tb could absorb the energy of secondary electrons produced by X-ray to generate ROS for significant tumor suppression (**Figure 3B**).

Yang *et al.* [146] proposed a novel QD-Photofrin conjugate for QD-based X-PDT, in which QD (CdSe core with a ZnS shell) was excited by X-ray and transferred energy to conjugated PS *via* fluorescence resonance energy transfer (FRET). The number of visible photons produced by the QD is linearly proportional to the radiation dose. The efficiency of FRET approached 100% when the Photofrin/QD ratio reached 291:1. *In vitro* assays proved that the combination of QD-Photofrin with X-ray resulted in enhanced H460 cell killing when compared with X-ray alone. Rossi *et al.* [147] used SiC/SiOx core/shell scintillating nanowire (ScNW)-conjugated tetra (4-carboxyphenyl) porphyrin (H₂TCPP) as a new PS system (SiC/SiOx-H₂TCPP) for silicon-based X-PDT. This SiC/SiOx-H₂TCPP could generate ¹O₂ when exposed to low-dose X-ray irradiation.

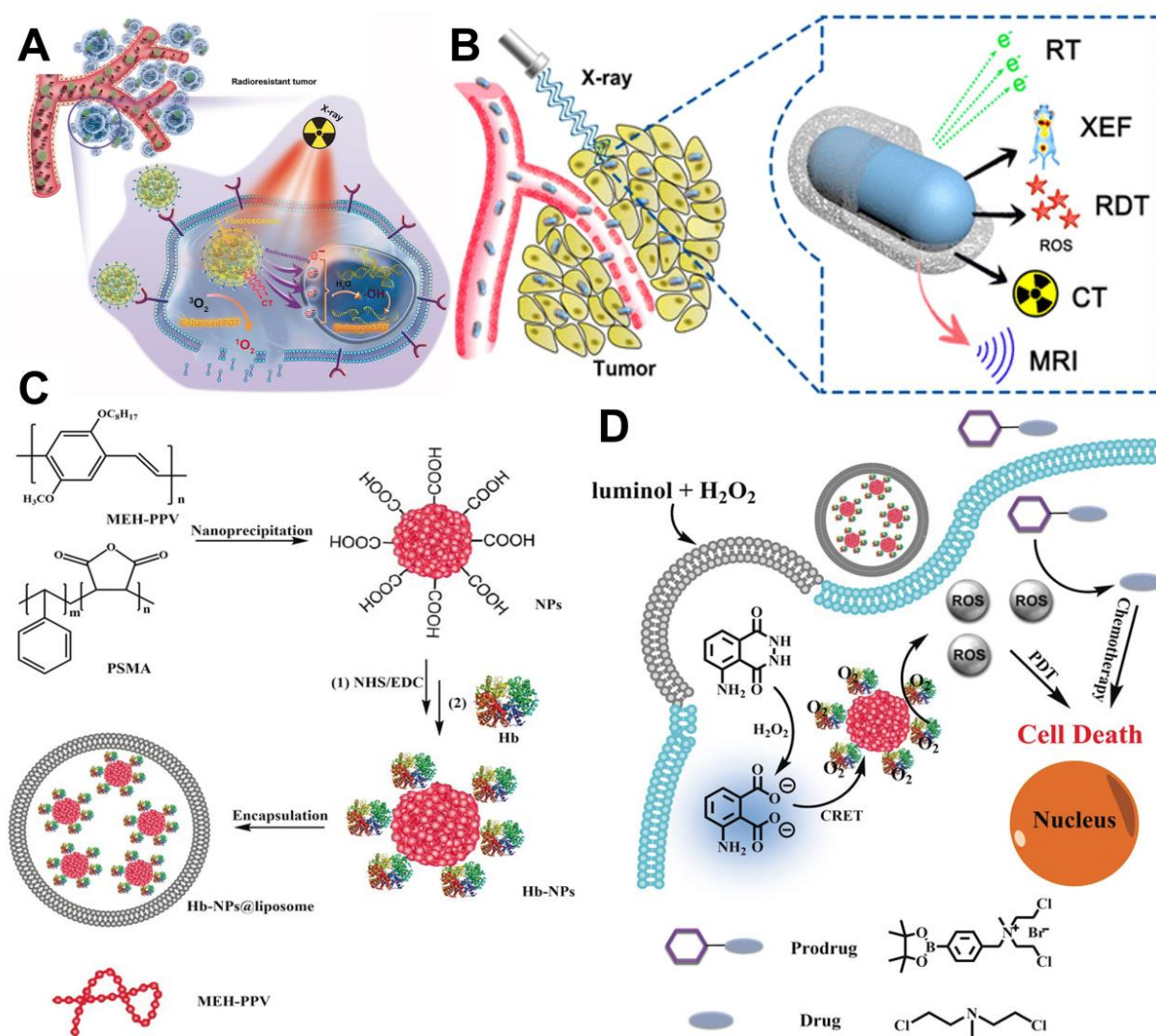


Figure 3. (A) Schematic representation of R-AIE-Au for fluorescence and CT imaging-guided X-ray-induced PDT. Reproduced with permission from Ref. [34], Copyright © 2019, Wiley-VCH Verlag GmbH & Co. KGaA, Weinheim. (B) Schematic illustration of X-ray activated NaCeF₄:Gd,Tb ScNPs for fluorescence/CT/MR imaging-guided PDT of cancer. Reproduced with permission from Ref. [35], Copyright © 2019, American Chemical Society. (C) Construction process of Hb-NPs@liposome. (D) Working model of the luminescing and O₂-supplying PDT system for cancer treatment. Reproduced with permission from Ref. [36], Copyright © 2019, Wiley-VCH Verlag GmbH & Co. KGaA, Weinheim. Abbreviations: PDT: photodynamic therapy; CT: computed tomography; MR: magnetic resonance; Hb: hemoglobin.

Moreover, the irradiation only took 20 s, which is shorter than the 40 s and 90 s used in standard clinical treatment.

Interstitial light

For deeply seated tumors in the body, interstitial PDT (I-PDT) is an alternative treatment which is usually performed by delivering light through multiple cylindrical diffusing fibers inserted into the target tumor. Shafirstein *et al.* [148] employed Photofrin®-mediated I-PDT to treat locally advanced head and neck cancers (HNC). I-PDT with Photofrin® significantly improved the cure rate compared to light (630 nm) delivery alone at the same irradiance and light dose. *In vivo* assays proved that local cures of VX2 were obtained in mouse tumors with I-PDT at 16.5–398 mW/cm² and ≥45 J/cm². In addition, the efficient delivery of therapeutic dose to target tumors with minimal damage to nearby intact tissues must be ensured for I-PDT to be used in deep tumors. For this purpose, Ismael *et al.* [149] adopted cylindrical diffuse optical fibers (CDFs) as the light source (630–760 nm) and optimized the output CDFs power to specify the light dose (20–50) J cm⁻² to the tumor site, thus achieving the effective treatment of breast cancer. Recently, Vermandel *et al.* [150] applied magnetic resonance imaging (MRI) as an estimator to assess the lesional effect of low-power 5-aminolevulinic acid (5-ALA)-based I-PDT. Based on the observations of MRI data and consideration of therapeutic effects, the 5-fraction light delivered at 5 mW during I-PDT is the most efficient treatment scheme with limited toxicity to adjacent healthy brain tissues, and might be a good way to comprehensively explore cell death pathways based on I-PDT.

Internal light

Considering that the external light source is limited by the light delivery efficiency, the research focus of light source in PDT further shifts from external light source to internal light source. For instance, Jiang *et al.* [36] prepared a PDT system by using hemoglobin (Hb)-linked conjugated polymer nanoparticles (CPNs) for the internal activation of PS. Specifically, in the presence of H₂O₂, Hb catalyzed the activation of luminol to produce chemiluminescence which could be absorbed by CPNs through chemiluminescence resonance energy transfer (CRET) to sensitize O₂, thereby generating ROS for cancer treatment (**Figure 3C and 3D**). In another example, Sun *et al.* [37] fabricated a luminescence PersLum material hydrogel (PLM-hydrogel) for high-efficient persistent luminescence-sensitized PDT. The PLM-hydrogel was synthesized by dispersing high-temperature calcined PLM into a biocompatible

alginate-Ca²⁺ hydrogel. It could be easily injected into tumor sites of mice as a powerful localized light source to trigger continuous ¹O₂ generation. *In vivo* tests effectively proved the persistent luminescence, light renewability, and strong fixing ability of PLM-hydrogel in tumors.

Summary of light source

In a short conclusion, for wider application of PDT, the availability, cost, and delivery efficiency of light source need to be considered, but the first priority is light penetration depth. Present innovative strategies based on NIR light, X-ray and internal light have solved this problem to a certain extent. Nevertheless, the low energy associated with NIR light, the weak PS activation ability and obvious side effects to normal tissues of X-ray, as well as the unsatisfactory energy transfer from internal light to PS remain challenging tasks. Recently, several new PDT excitation sources, including microwaves [130], radio-waves [131], ultrasound [132], electrical fields (EF) [133], and magnetic fields (MF) [134], have emerged and made some progress. Microwave irradiation can cause local hyperthermia and increase the blood supply to the tumor. Ultrasound can penetrate deep into the tumor to activate PSs. The electroporation effect of EF can help PSs pass through the cell membrane. MF can realize the magnetic target accumulation of PSs. Future study of the above excitation sources is encouraged.

Photosensitizers (PSs)

PSs play a critical role in the therapeutic effect of PDT. Ideally, the most suitable PSs for PDT are adjustable amphiphilic reagents in biological environments. These PSs should exhibit strong molar absorption of long-wavelength light and be non-toxic when not exposed to light. They should also have a long triplet lifetime and an excellent ¹O₂ quantum yield [38–40]. Ideal PSs should target tumor tissues with long-term retention and then can be rapidly removed from the body after the end of treatment. A great deal of work has been carried out in recent years to develop various PSs for PDT. In this part, we will first introduce the types of PSs, and then discuss the innovative research to enhance ROS generation ability, solubility and targeted ability of PSs.

Types of PSs

In the last few decades, a large number of organic and inorganic PSs used in PDT have been developed for cancer treatment. The organic PSs used in clinical or preclinical applications of PDT includes porfimer sodium, 2-(1-hexyloxyethyl)-2-devinyl pyropheophorbide-a, verteporfin, temoporfin, silicon

phthalocyanine 4, porphyrin, redaporfin, talaporfin, photolon (chlorin e6 (Ce6) sodium-polyvinylpyrrolidone), hemoporphin, padeliporfin, photodithazine, photosens, hiporfin, photocyanine, and radachlorin [30]. Hematoporphyrin derivative (HpD), dihaematoporphyrin ether (DhE), and photofrin porfimersodium are the first generation organic PSs widely used for PDT [41]. Although they have been approved by the Food and Drug Administration (FDA), their production and efficacy is limited by the complex synthesis process, immature purification technology, and low molar extinction coefficient [42-46]. As a result, the second generation PSs with high $^1\text{O}_2$ yields are developed, which includes phthalocyanines (zinc phthalocyanine (ZnPc)) [47], bacteriochlorins [48], hypericin [49], phenothiazines (methylene blue (MB) and toluidine blue) [50], cyanines (merocyanine-540) [51], metalloporphyrins [29], xanthenes (rose Bengal (RB)) [53], and porphycenes [54]. Nevertheless, the clinical use of these PSs is also hampered by the targeting and stability issues. To enhance the tumor targeting ability, third generation PSs conjugated with targeted agents are synthesized, such as Ac-L-Phe-ALA-OME, galactose substituted Si(IV)-phthalocyanine and sugar conjugated chlorins [55]. In addition, a number of new PSs have emerged, including indocyanine dyes (indocyanine green (ICG), IR-825, and IR-780), BODIPYs, diketopyrrolopyrrole (DPP), aggregation-induced emission (AIE) dyes, curcumin, perylenequinone, furocoumarin, noble metal complexes (Ru(II)/Ir(III)/Au(III) complexes), organic frameworks compounds (MOFs, covalent organic frameworks (COFs), hydrogen-bonded organic frameworks (HOFs)), and polymer-based PSs (polyfluorene, polythiophene) [151]. However, the targeting efficiency or *in vivo* selectivity of them is not high enough for clinical use. Hence, greater efforts should be devoted to designing PSs with strong stability and targeted ability.

In recent years, increasing attention has been paid to the research of inorganic PSs based on nanomaterials. Generally, nano-inorganic PSs contain gold nanoparticles [56], silver nanoparticles [57], porous silicon nanoparticles [58], CdTe quantum dots (QDs) [59], carbon materials [60], black phosphorus (BP) [61], titanium dioxide (TiO_2) [62], transition metal oxides (TMOs) heterojunction [63], Ti_3C_2 nanosheets [64], and graphitic-phase carbon nitride ($g\text{-C}_3\text{N}_4$) nanosheets [65]. Compared with organic PSs, nano-inorganic PSs are more potent for PDT for several reasons. First, most inorganic PSs are stable even under laser irradiation. Second, the modification and functionalization of inorganic PSs endow them with targeting ability, which is beneficial to the

realization of precise cancer treatment and reduction of side effects. Last, some inorganic PSs are widely utilized as carriers of photothermal reagents and chemotherapeutic drugs, allowing for the synergistic treatment of multiple therapeutic approaches. However, the inherent disadvantages of inorganic PSs such as low $^1\text{O}_2$ quantum yield, poor biodegradability and biosecurity largely hinder their clinical application. More attempts are therefore needed to address these limitations.

Enhanced stability and targeting ability of PSs

Most organic PSs are highly hydrophobic and tend to aggregate in aqueous environments. The aggregation process can reduce the therapeutic efficiency of PDT since PSs must remain in monomer form to be photoactive [151]. This monomer structure can be achieved by combining PSs with nanomaterials. For example, covalent bonding with hydrophilic polymer molecules can effectively enhance the bioavailability of hydrophobic porphyrins [152]. Thus, using nano-sized carriers to deliver PSs can be a feasible strategy to improve the poor stability of traditional organic PSs. Zhang *et al.* [66] utilized thermal responsive phase change materials (PCM) as carriers to co-encapsulate ultrasmall manganese dioxide ($s\text{MnO}_2$) and organic PSs (IR780) for tumor hypoxia-modulated PDT. The protective PCM layer not only effectively prevented the photodegradation of IR780 but also endowed IR780 with better solubility than free IR780 (**Figure 4A**). Meanwhile, the PCM layer could immediately release $s\text{MnO}_2$ under laser irradiation, which further triggered the decomposition of endogenous H_2O_2 to generate enough O_2 for relieving tumor hypoxia (**Figure 4B**). *In vivo* photoacoustic (PA) and fluorescence imaging illustrated that IR780- $s\text{MnO}_2$ -PCM nanoparticles (NPs) could accumulate in tumors and showed efficient tumor retention under intravenous injection. As revealed by *in vivo* PDT treatments, IR780- $s\text{MnO}_2$ -PCM NPs displayed superb performance in inhibiting tumor growth.

Recently, naturally derived nanocarriers, including exosomes (Exos) and platelets, have been attracting more attention than other nanocarriers and applied to therapeutics owing to their transcellular permeability and biocompatibility [67,68]. For example, Pan *et al.* [69] adopted high-purity urinary Exos to load amphiphilic polymer (PMA)-coated/Au-BSA@Ce6 NPs. In this Exo-PMA/Au-BSA@Ce6 system, the presence of Exos successfully improved the hydrophobicity and poor biocompatibility of Ce6, resulting in enhanced PDT performance with abundant $^1\text{O}_2$ generation. Meanwhile, this Exo-based nanocarrier could penetrate through the membrane

barrier and target tumor tissues, thus achieving targeted PDT with deep penetration and superior tumor retention (Figure 4C–4G).

In terms of tumor targeting, surface modification of PSs with targeting ligands or moieties can effectively achieve tumor-targeted accumulation of PSs. Wang *et al.* [70] employed cancer cell membrane (CM) to enhance the tumor-targeted accumulation of PSs. Specifically, PS (Ce6) was embedded with magnetic mesoporous organosilica nanoparticles (M-MONs) and then covered with breast cancer cell membrane (CM@M-MON@Ce6) for PDT (Figure 5A). The homologous targeting effect caused by the affinity between the adhesion molecules on the breast cancer cell membrane and their source cells facilitated the favorable tumor-targeted accumulation of CM@M-MON@Ce6 with prolonged blood circulation time. The therapeutic efficacy of CM@M-MON@Ce6 was evaluated by animal experimentation, and the results illuminated that this PDT nanoplatform possessed a remarkable eradication effect on primary tumors.

In another strategy, Cheng *et al.* [71] proposed an amino acid modification strategy to regulate the intracellular distribution of PS (protoporphyrin IX (PpIX)) for targeted PDT. In this platform, the membrane anchoring ability and phototoxicity of

PpIX to different cell lines could be effectively controlled at the level of single arginine (Figure 5B and 5C). Systematic studies indicated that the obtained nanoplatform (Ac-K(PpIX)-En) possessed excellent biocompatibility and targeting ability. *In vitro* and *in vivo* assays confirmed the robust anti-tumor effect of Ac-K(PpIX)-En with low biotoxicity. In addition, glycopolymers can also be used as targeting ligands. Sun *et al.* [153] developed a conjugated polymer-based PS (PPF-Ir-g-(POEGMA-*b*-PGal)), in which a PS Ir (III) complex was covalently attached to the conjugated backbone (poly(benzene-*alt*-fluorene), PPF-Ir), and a water-soluble polymer (POEGMA-*b*-PGal) was further grafted from the PPF-Ir. The brush structured PPF-Ir-g-(POEGMA-*b*-PGal) exhibited excellent water solubility and targeting ability since glycopolymer polygalactose (PGal) can specifically bind to asialoglycoprotein receptor (ASGPR) overexpressed on the surface of HepG2 cells. In an *in vitro* assay, this polymer-based PS damaged HepG2 cancer cells under white light irradiation. Moreover, xenograft HepG2 tumors were significantly inhibited *in vivo*.

Enhanced ROS generation efficiency of PSs

In addition to improving the stability and targeting of PSs, further advancements on ROS generation efficiency are still required. $^1\text{O}_2$ generation

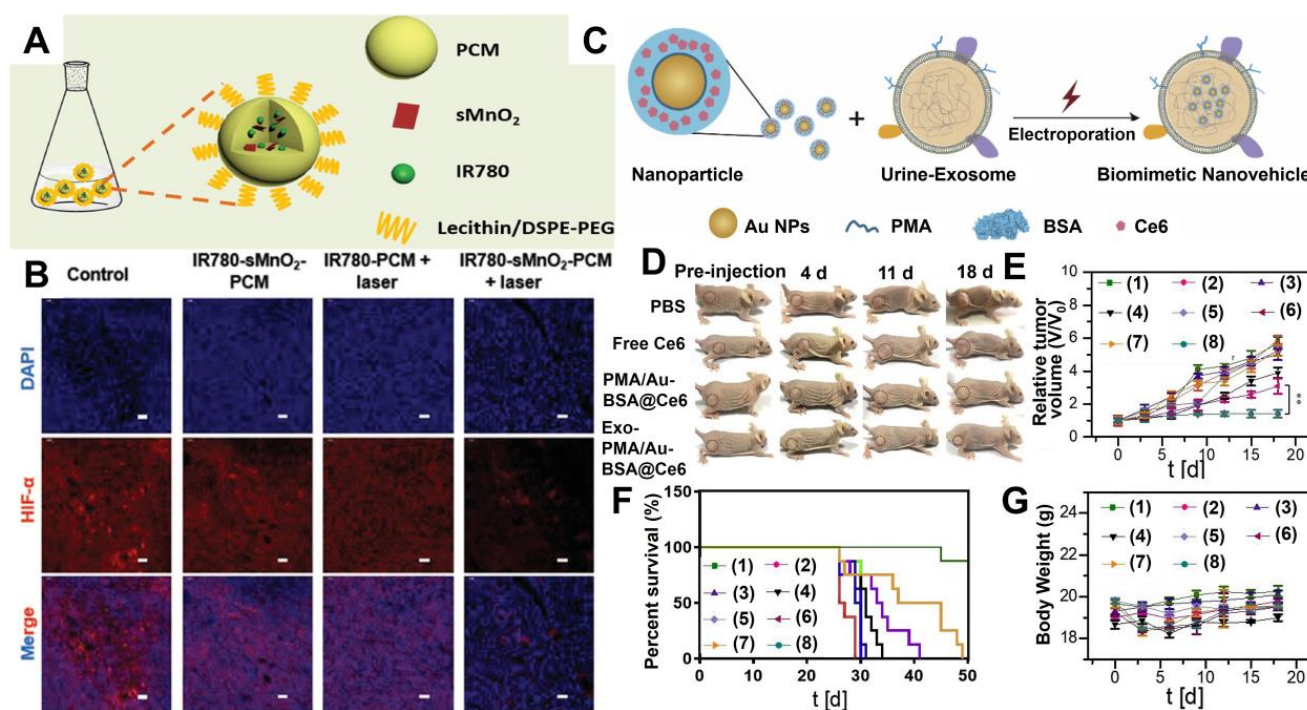


Figure 4. (A) Synthetic schematic of IR780-sMnO₂-PCM nanoparticles. (B) Immunofluorescence staining of HIF-1 α under different conditions. Reproduced with permission from Ref. [66], Copyright © 2019, Wiley-VCH Verlag GmbH & Co. KGaA, Weinheim. (C) Schematic illustrations of the preparation of Exo-PMA/Au-BSA@Ce6 nanovehicles for targeted PDT. (D) Tumor growth of mice after different treatments for 18 days. (E) Tumor volumes curves, (F) survival rates, and (G) body weight of mice after different treatments: (1) PBS; (2) PBS+laser; (3) free Ce6; (4) free Ce6+laser; (5) PMA/Au-BSA@Ce6; (6) PMA/Au-BSA@Ce6+laser; (7) Exo-PMA/Au-BSA@Ce6; (8) Exo-PMA/Au-BSA@Ce6+laser. Reproduced with permission from Ref. [69], Copyright © 2019, Elsevier. Abbreviations: PCM: phase change materials; Exo: exosomes; PMA: amphiphilic polymer; Ce6: chlorin e6; PDT: photodynamic therapy.

quantum yield can be used as an index to evaluate the photodynamic effect of type II-based PSs. To optimize the ROS generation of PSs, ISC rate constant can be increased by incorporating heavy atoms (N, Br, Pt, Hf, thiophenyl group, etc.) or 2,2,6,6-tetramethylpiperidinyloxy (TEMPO) to PSs, reducing the energy gap (ΔE_{ST}) between S_1 and T_1 , or introducing electron-withdrawing/-donating groups in the conjugated structure [29]. For example, Zhou *et al.* [154] combined Ru(II) polypyridyl complex with Pt(II)-based supramolecular coordination complexes to form heterometallic metallacycle Ru-Pt for NIR-activated PDT. The obtained Ru-Pt exhibited a high 1O_2 generation quantum yield (89%) owing to the heavy atom effect of Pt. *In vivo* assays confirmed that Ru-Pt could effectively inhibit tumor growth under low light dose irradiation. In addition to the heavy atom effect, TEMPO can also increase the ISC rate through radical-triplet pair mechanism. By incorporating TEMPO into Cy7 dyes, the as-prepared dye compound (dye 2) displayed a higher 1O_2 generation quantum yield than Cy 7 (20% vs 0.6%) [155]. A low ΔE_{ST} can lead to a high ISC rate and promote the energy transfer from $^3PS^*$ to O_2 , thus

decreasing the ΔE_{ST} of PS can be an efficient way to increase 1O_2 quantum yield. Shi *et al.* [156] successfully synthesized two DPP derivatives, phenyl-substituted DPP (PDPP) and thienyl-substituted DPP (TDPP). The ΔE_{ST} values of PDPP and TDPP are calculated to be 0.66 and 0.48 eV, respectively. Both *in vitro* and *in vivo* experiments proved that TDPP performed better in generating 1O_2 to kill cancer cells and eliminate tumor than PDPP. In addition, the electron-withdrawing and electron-donating groups can affect the energy level of complexes and facilitate the ISC process. For example, a coumarin-modified Ru(II) PS (Ru2) shows lower oxidation potential and higher extinction coefficient than a coumarin-free Ru(II) PS, resulting in improved ROS generation efficiency [118]. A series of push-pull AIEgens synthesized by coupling diphenylamine group with different electron-withdrawing groups on carbazolyl rings also exhibit enhanced 1O_2 generation capability [157]. For the semiconductor nanomaterials, the ROS generation efficiency can be improved by optimizing their size, morphology, heteroatom doping, and surface state.

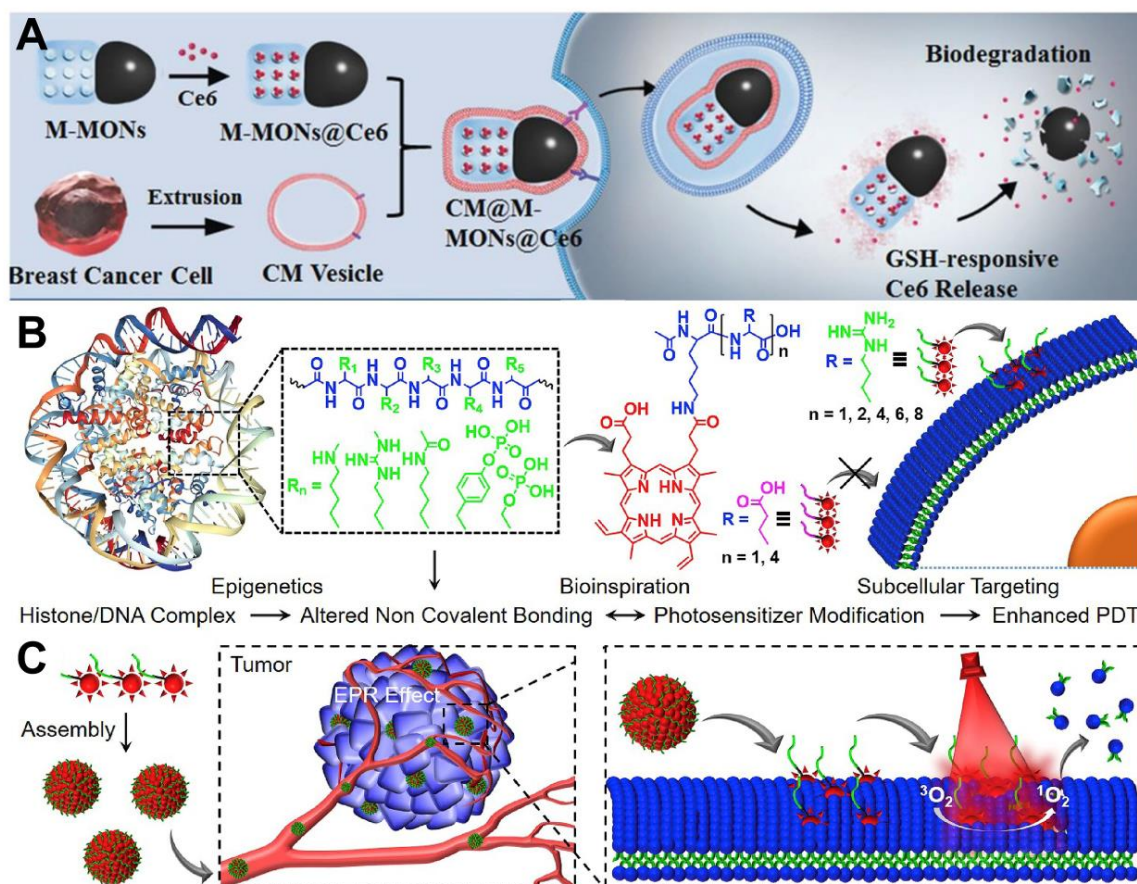


Figure 5. (A) Schematic illustration of the preparation of CM@M-MON@Ce6 for PDT. Reproduced with permission from Ref. [70], Copyright © 2019, Wiley-VCH Verlag GmbH & Co. KGaA, Weinheim. (B) Chemical structures of amino acids modified PpIX and schematic illustration of plasma membrane-targeted PDT. (C) Tumor targeted delivery of Ac-K(PpIX)-En for PDT-induced plasma membrane rupture. Reproduced with permission from Ref. [71], Copyright © 2019, Elsevier. Abbreviations: CM: cell membrane; Ce6: chlorin e6; PDT: photodynamic therapy; PpIX: protoporphyrin IX.

Table 1. Some commonly used nanocarriers and conjugates for PDT

Nanocarriers	Loaded PSs	Ref.	Conjugates	Targeted tumor/cancer cells	Ref.
SiO ₂ NPs	Purpurin-18, HpD, hypocrellin A, chlorin, MB, PPHP and ZnPc	[16,72]	Breast cancer cell membrane	Breast cancer cells	[70]
Liposomes	m-THPC	[74]	Arginine	Plasma membrane	[71]
Micelles	PpIX	[75]	Folic acid	Cell surface folate receptors	[88]
Carbon nanomaterials	ICG, Ce6, porphyrin	[76,79]	Phenylalanine	Transformed PAM212 keratinocyte cells	[89]
Peptide-Based nanoparticles	Phthalocyanine	[77,141]	Retinoic acid	Neuroblastoma SK-N-DZ cells surface retinoic acid receptors	[90]
Bacteriophage nanowires	Pyropheophorbide a	[78]	Glucose and galactose	K562 cells	[91]
Polymer	Ce6, MB, m-THPC, PpIX, graphitic carbon nitride quantum dots	[81,98]	Low-density lipoprotein	Colon, HepG2 and retinoblastoma tumors	[92]
Exosomes	Ce6	[67,69]	Magnetoliposomes	Melanoma	[93]
Phase-change materials	IR780	[66]	Epidermal growth factor	Breast carcinoma cells, epidermal carcinoma and ovarian cancer	[94]
LDHs	ZnPc, Ce6, ICG	[33,83]	Monoclonal antibodies	Ovarian and breast cancer cells	[95]
MOFs	Ce6, ICG	[80,84]	Human serum albumin	Breast cancer cells	[96,140]
2D transition metal dichalcogenides (TMDs)	Ce6, MB	[85,173]	RGD (Arg-Gly-Asp)	HepG2	[112]
Mesenchymal stem cells	Purpurin-18	[73]	Triethylene glycol (TEG)	Breast cancer cell surface protein	[123]
MnO ₂	Silicon phthalocyanine dihydroxide, Ce6, TiO ₂	[86,174]	(4-carboxybutyl)triphenylphosphonium bromide	Mitochondria	[97]
			Hyaluronic acid (HA)	Cell surface CD44 receptor	[63]
			Glycopolymers	The asialoglycoprotein receptor (ASGPR) overexpressed on the surface of HepG2 cells	[153]

Summary of PSs

In brief, a great many of PSs for PDT have been developed over the last few decades. The latest knowledge indicates that the modification of PSs using nanocarriers and targeting conjugates can significantly enhance their water-solubility, targeting and delivery efficiency. In addition to phase change materials, exosomes, cancer cell membrane and amino acids, some commonly used nanocarriers and targeting conjugates in other strategies are summarized in Table 1. Nevertheless, it is still complicated and challenging to improve the stability, solubility, and tumor targeted ability of PSs since their morphology, particle size, and surface modification can significantly affect the stability and tumor-targeting ability. In addition, it is worth noting that targeting is an extensively studied but unproven concept that has been around for a long time, so it may be unlikely to translate into clinical practice. More efforts are needed in the research of PSs to facilitate the clinical application of PDT.

Oxygen dependence

Most existing PDT systems are in the form of

type II mechanism that involves significant O₂ consumption. However, inadequate O₂ concentration is a characteristic feature of many solid tumors, which significantly hampers the antitumor effect of PDT [98]. To deal with tumor hypoxia, great efforts have been made in recent years and many innovative strategies have been proposed. Based on the mechanisms responsible for PDT process, these innovative strategies can be classified into three categories: (1) O₂-replenishing strategies that can increase tumor O₂ concentration by direct or indirect means; (2) O₂-independent strategies that can perform PDT even under low O₂ conditions; (3) O₂-economized strategies that can block intracellular O₂ consumption. In this section, we will discuss in detail these three categories of PDT innovative strategies dedicated to overcoming tumor hypoxia.

O₂-replenishing strategies

Delivery of O₂ into the tumor

Direct delivery of O₂ into tumor with appropriate O₂ carriers is one of the most common strategies to overcome tumor hypoxia in PDT. Commonly used O₂ carriers include Hb,

perfluorocarbons (PFCs) and MOFs. The O₂ carrying capacity of Hb makes it an attractive candidate for reoxygenation. Considering the poor stability and short circulation time of Hb, artificial red blood cells (RBCs) are combined with Hb to conquer the defects of free Hb [99]. For example, Luo *et al.* [100] fabricated artificial RBCs to load Hb and ICG for O₂-supply PDT. Similar to natural RBCs, these Hb-contained artificial RBCs could reversibly bind to four O₂ molecules to form HbO₂ (Figure 6A), thus enabling the stable self-enrichment of O₂ for subsequent massive ROS generation. Importantly, Hb could be oxidized into highly oxidative ferryl-Hb species, leading to the synergistic oxidative damage of xenograft tumor. Other Hb-related O₂ carrier systems have also been investigated, such as liposomes and polymeric micelles [101]. However, since each Hb molecule can only bind to four O₂ molecules, these systems are limited to a certain extent by O₂ loading ability.

To achieve a high O₂ delivery, PFCs can be an excellent choice thanks to the high electronegativity of fluorine atoms that endows PFCs with excellent O₂ affinity. Consequently, PFCs are utilized as important components of O₂ delivery systems to surmount hypoxia and improve the effectiveness of PDT in cancer therapy [102]. Cheng *et al.* [103] developed a

novel O₂ self-enriched PDT system (Oxy-PDT) by loading a PS (IR780) into PFCs nanodroplets (Figure 6B), in which a sufficient O₂ concentration was maintained. Both *in vitro* and *in vivo* tests confirmed the enhanced therapeutic efficacy of Oxy-PDT, which was attributed to the high O₂ availability for ¹O₂ generation in Oxy-PDT. Moreover, the half-life of ¹O₂ in PFCs was 5×10^{-2} s, which is much longer than that in the cellular environment (6×10^{-7} s) or water (5×10^{-6} s), resulting in long-lasting PDT effect. Similarly, Zhang *et al.* [158] synthesized a poly(ethylene glycol)-boron dipyrromethene amphiphile (PEG-F₅₄-BODIPY) with 54 fluorine-19 (¹⁹F), and employed it to emulsify perfluorohexane (PFH) into a nanoemulsion (PFH@PEG-F₅₄-BODIPY). The as-prepared nanoemulsion significantly enhanced the therapeutic effect of BODIPY by dissolving O₂ and reducing the self-quenching of BODIPY molecules. *In vitro* and *in vivo* assays indicated that PFH@PEG-F₅₄-BODIPY could effectively alleviate tumor hypoxia through the O₂ storage capability of PFH.

MOFs are a new kind of porous nanomaterials with ultrahigh surface areas and uniform pore sizes. The use of MOFs as O₂ storage/carrying nanomaterials for hypoxia modulation has been extensively investigated [104]. Recently, Gao *et al.* [80]

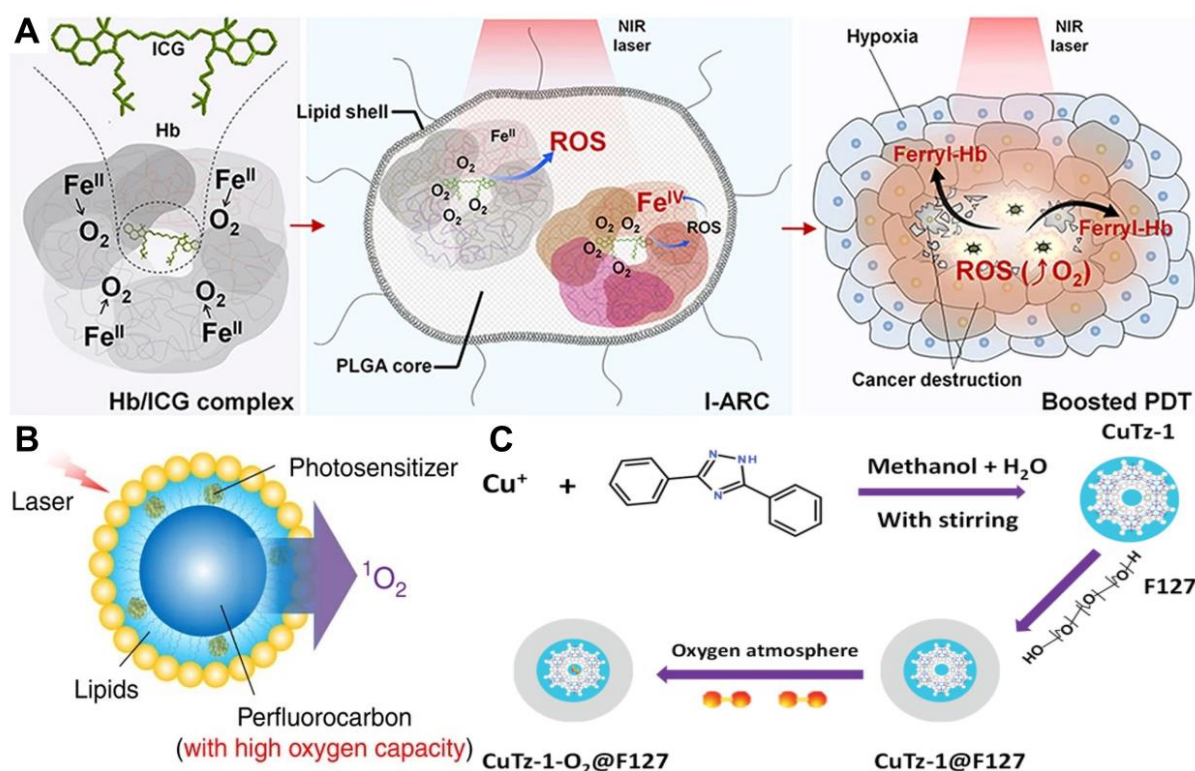


Figure 6. (A) Schematic illustration of PS system based on Hb and ICG co-loaded RBCs for tumor-boosted PDT. Reproduced with permission from Ref. [100], Copyright © 2016, Nature Publishing Group. (B) Schematic of PFCs internalized Oxy-PDT agent for tumor inhibition. Reproduced with permission from Ref. [103], Copyright © 2015, Nature Publishing Group. (C) Schematic of the synthetic procedure of CuTz-1-O₂@F127 for enhanced PDT. Reproduced with permission from Ref. [105], Copyright © 2019, Wiley-VCH Verlag GmbH & Co. KGaA, Weinheim. Abbreviations: Hb: hemoglobin; ICG: indocyanine green; RBCs: artificial red blood cells; PDT: photodynamic therapy; PFCs: perfluorocarbons.

utilized the significant gas-storage capability of zirconium (IV)-based MOFs (UiO-66) to realize O₂-evolving PDT. As a carrier for O₂ storing, UiO-66 was conjugated with PS (ICG) through coordination reaction and further encapsulated in RBCs membranes to construct a PDT nanoplatfrom (O₂@UiO-66@ICG@RBC). The O₂ isotherms demonstrated that the O₂ storage capacity of UiO-66 reached 500 μmol g⁻¹ and the stored O₂ was effectively released under NIR light irradiation. Owing to the long circulation and O₂ self-sufficiency of MOFs, the designed nanoplatfrom displayed an enhanced efficiency of tumor ablation. In another work, Cai *et al.* [105] designed a biodegradable O₂-loaded MOF therapeutic platform (CuTz-1-O₂@F127) (**Figure 6C**). The O₂-loaded CuTz-1@F127 could accumulate in the tumor due to the enhanced permeability and retention (EPR) effect and release the absorbed O₂ at the tumor site. The high antitumor efficacy of this O₂-evolving PDT platform was successfully demonstrated by *in vitro* and *in vivo* studies.

In situ O₂ generation

There are three strategies to produce O₂ *in situ*: (1) H₂O₂-decomposition triggered O₂ generation; (2) water-splitting mediated O₂ generation; (3) photosynthetic O₂ production. For the first way, considering the high H₂O₂ level in TME, *in situ* O₂ generation inside tumor by catalyzing the decomposition of H₂O₂ can be an effective strategy to overcome tumor hypoxia [106]. For the second mode, inspired by the nature, scientists have developed photocatalytic reactions to generate O₂ from H₂O [107]. For the third manner, it is generally believed that O₂ molecules come from primitive photosynthesis of microorganisms (cyanobacteria and archaea) [108], which can photosynthesize to produce O₂ using the photosystem on the thylakoid membrane.

In the H₂O₂-decomposition triggered O₂ generation strategy, catalase [109] and inorganic nanomaterials based on calcium (Ca), gold (Au), platinum (Pt), manganese (Mn), Ce and copper (Cu) are widely used to catalyze H₂O₂ decomposition in recent years [106]. For instance, Chen *et al.* [110] constructed an intelligent H₂O₂-responsive and O₂-evolving nanosystem based on MnO₂ nanoparticles (HSA-MnO₂-Ce6&Pt NPs) to overcome the tumor hypoxia-associated resistance of PDT. In this nanosystem, MnO₂ could generate O₂ *in situ* by reacting with endogenous H₂O₂ inside TME (**Figure 7**). Yao *et al.* [111] proposed synergetic mesoporous cerium oxide upconversion nanoparticles (Ce-UCNPs) to achieve the pH/H₂O₂-responsive

self-sufficiency of O₂. Cerium oxide NPs can reversibly switch from Ce⁴⁺ to Ce³⁺ and simultaneously catalyze H₂O₂ to O₂ due to their enzyme-like activity [112]. *In vivo* tests demonstrated that the Ce-UCNPs could efficiently decompose the intracellular H₂O₂ to generate sufficient O₂, successfully overcoming hypoxia. Another strategy for designing O₂-supply PDT platforms is to use Pt NPs. Liang *et al.* [81] prepared a nano-multifunctional platform (PDA-Pt-CD@RuFc) by loading Pt-modified and cyclodextrin (CD)-decorated polydopamine (PDA) NPs with a Ruthenium (II) complex (RuFc). The Pt NPs catalyzed the generation of O₂ from H₂O₂, and then RuFc photoactivated O₂ to produce ¹O₂ for PDT. This nanoplatfrom successfully overcame the tumor hypoxia.

For water-splitting mediated O₂ generation strategy, carbon nitride (C₃N₄)-based multifunctional nanocomposite (PCCN) was prepared by Zheng and co-workers [107] for light-driven water splitting, in which carbon dot-doped C₃N₄ was assembled with PS (PpIX) *via* π-π stacking. In this nanosystem, the water-splitting efficiency of C₃N₄ alone is limited, but the use of carbon dots to enhance the red light absorption could improve its water-splitting efficiency under 630 nm laser irradiation, ultimately increasing the intracellular O₂ concentration. Subsequently, PpIX transmitted the energy to the produced O₂ to generate ¹O₂ under a 630 nm laser (**Figure 8A**). *In vitro* and *in vivo* assays indicated that this PCCN nanosystem possessed excellent capability to improve the intratumoral O₂ level. Compared with 630 nm laser, NIR can penetrate into deeper tissues with lower scattering and absorption. On this basis, Li *et al.* [113] reported iron-doped C₃N₄ (Fe-C₃N₄) and the ability of water-splitting mediated O₂ generation was also demonstrated. Ru (II) complex (Ru(bpy)₃²⁺) as a PS was loaded onto Fe-C₃N₄ to form Fe-C₃N₄@Ru@HOP (FCRH) nanocomposite. Since the Ru (II) complex could be excited by simultaneous absorption of two photons of NIR light, a two-photon laser was used to activate O₂ production through Fe-C₃N₄ and ¹O₂ generation by Ru(bpy)₃²⁺ to provide appropriate synchronization for the two processes (**Figure 8B-8D**).

In the photosynthetic O₂ production strategy, microorganism-based PDT for hypoxic tumor therapeutics was reported [114]. Huo *et al.* [115] fabricated a photosensitive and photosynthetic cyanobacteria-based PDT system (ceCyan cells) by encapsulating PSs (Ce6) inside the *Synechococcus elongatus* PCC 7942 (Cyan). Under 660 nm laser irradiation, the ceCyan cells generated O₂ through photosynthesis, and Ce6 activated the O₂ into ¹O₂. The cascade process could produce large amounts of ¹O₂

to destroy cancer cells both *in vitro* and *in vivo* with a single-wavelength laser light source. Considering that photosynthetic bacteria (*Synechococcus* 7942, Syne) possess stronger tumor targeting ability than Cyan, Liu *et al.* [116] utilized Syne as the PS carrier and *in situ* photocatalyzed O_2 generation to realize photosynthesis-boosted PDT (Figure 9A). ICG-encapsulated NPs (HSA/ICG) were assembled and then connected with the surface of Syne *via* amide bonds to form a PDT system (S/HSA/ICG). The photoautotrophic Syne not only promoted the delivery of ICG into the tumor through its intrinsic targeting ability, but also increased the intratumoral O_2 concentration through photosynthesis under the irradiation of 660 nm laser, thus improving the therapeutic efficacy of PDT. Upon intravenous injection, S/HSA/ICG effectively accumulated in the tumor site and generated abundant O_2 continuously under laser irradiation (Figure 9B), which remarkably ameliorated tumor hypoxia and boosted ROS production. It should be pointed out that although the

above researches have effectively demonstrated the ability of photosynthetic bacteria to produce O_2 *via* photosynthesis, the O_2 generation efficiency has not been studied, and more efforts are needed.

O_2 -independent strategies

Apart from O_2 -replenishing strategies, new paradigms involving diminished O_2 dependence are also favored in PDT. As described above, type I mechanism is an electron transfer process utilized in PDT systems. It can produce toxic free radicals including $\cdot OH$ and $\cdot O_2^-$ under laser irradiation. Studies show that type I PDT performs well even at low O_2 concentrations, which lays foundation for designing new approaches to break through the hypoxia limitation of type II PDT [117]. In a recent work by Lv *et al.* [118], a coumarin-modified cyclometalated Ru(II) PS (Ru2) exhibited excellent type I PDT effect. The successful modification of Ru(II) complex by coumarin enhanced the light-absorption ability of Ru2 in the visible region

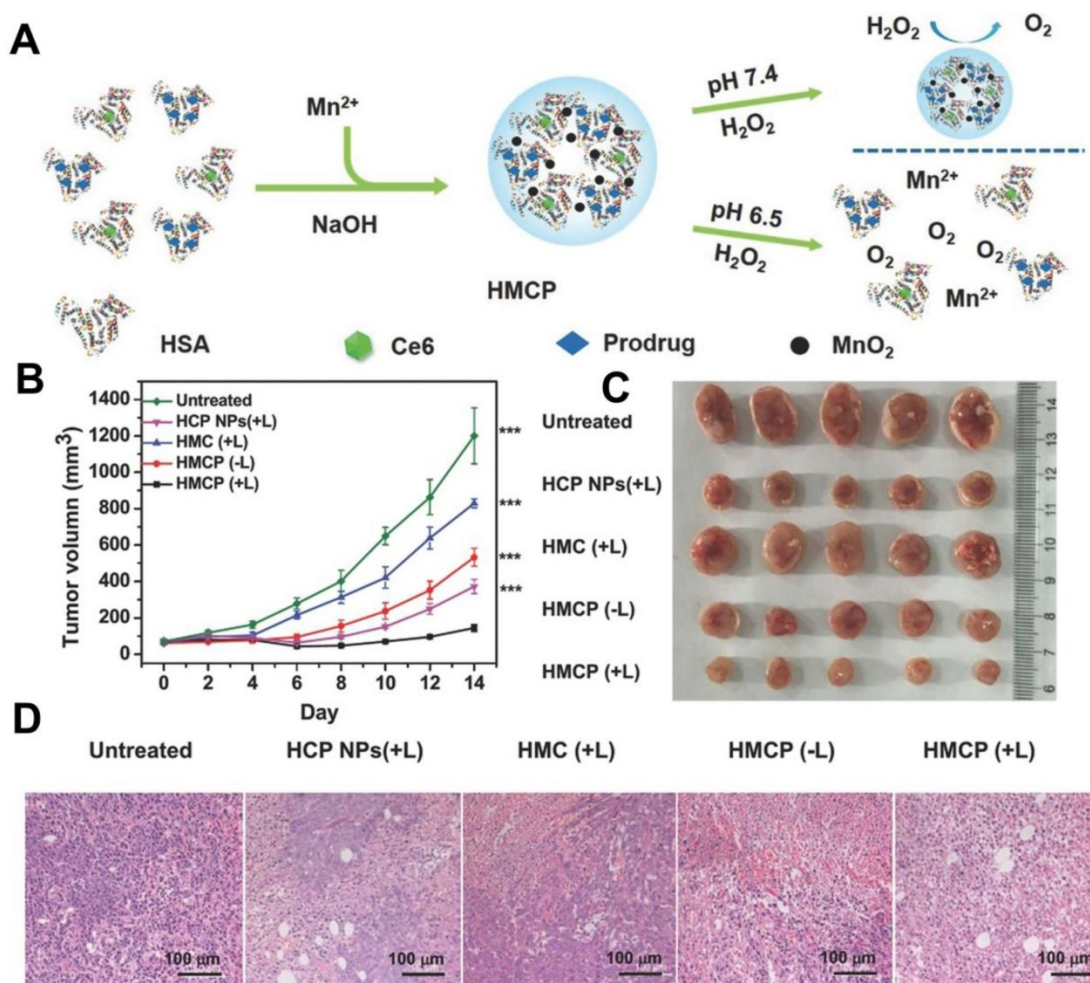


Figure 7. (A) Schematic illustration of the fabrication of HSA-MnO₂-Ce6&Pt nanoparticles. (B) Tumor volume curves of mice on day 14 after various treatments, and (C) corresponding photographs of tumors collected from mice at the end of treatment. (D) H&E staining assay of tumor slices from different groups of mice collected 24 h after 661 nm light irradiation. Reproduced with permission from Ref. [110], Copyright © 2016, Wiley-VCH Verlag GmbH & Co. KGaA, Weinheim. Abbreviations: Ce6: chlorin e6; H&E: hematoxylin and eosin.

(400–800 nm). The PDT effect was evaluated under both normoxia and hypoxia conditions, and the results showed that Ru2 maintained superior PDT activity even under hypoxia (**Figure 10A–10D**), which could be attributed to the direct electron transfer between the excited Ru2 and the adjacent substrates through the photochemical process of type I.

In another work, Lan *et al.* [119] demonstrated a new MOF-based PDT system (Ti-TBP) consisting of Ti-oxo chain secondary building units (SBUs) and 5,10,15,20-tetra (p-benzoato) porphyrin (TBP, a kind of PSs), which could be used for hypoxia-tolerant type I PDT. Upon 650 nm light irradiation, Ti-TBP transferred electrons from excited TBP* to Ti-oxo chain SBUs to produce TBP^{•+} and Ti³⁺ species, which induced the generation of OH and O₂⁻ (**Figure 10E**), and thus elicited superb anticancer effect of type I PDT with a tumor suppression rate of 98%. Similarly,

Bevernaegie *et al.* [120] developed photo-oxidizing iridium(III)-based sensitizers (Ir(III)) to damage hypoxic tumors through type I mechanism under oxygen-free conditions. Viability assays were performed on 3D tumor spheroids under both normoxic and hypoxic conditions, and the corresponding results proved that Ir(III) could penetrate deeply into 3D tumor spheroids and destroyed them completely under 405 nm light irradiation even at low O₂ concentrations.

Recently, Li *et al.* [121] proposed a nanostructured 2,4,6-tris-(N,N-dimethylamino-methyl)phenoxy substituted Zinc(II) phthalocyanine assembly (NanoPcA) that could trigger ROS generation *via* type I mechanism. In this PDT system, the NanoPcA possessed high electron-donating ability which is conducive to promoting type I photoreactions. Moreover, the electron-rich surface of

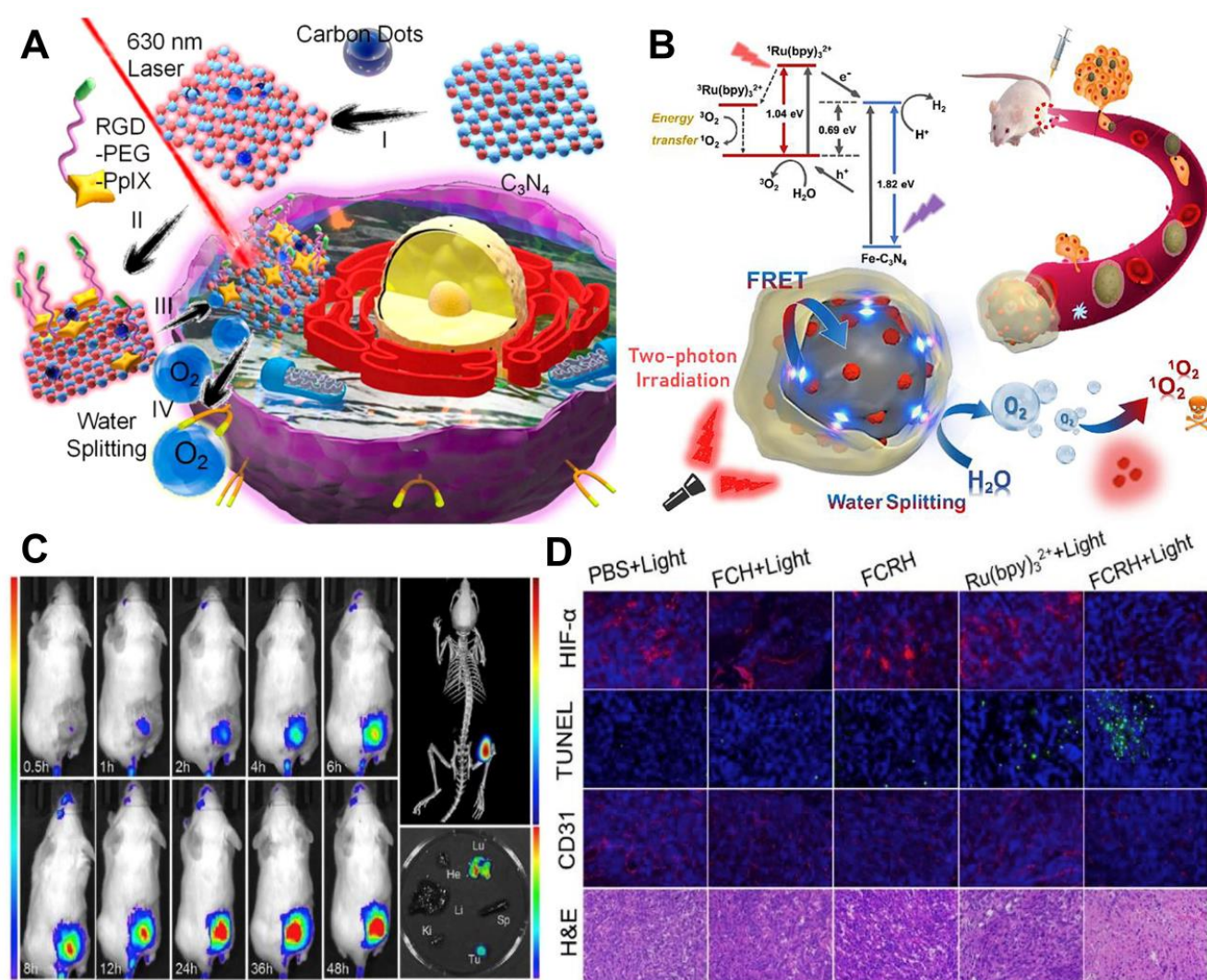


Figure 8. (A) Schematic illustration of PCCN-mediated water splitting enhanced PDT. Reproduced with permission from Ref. [107], Copyright © 2016, American Chemical Society. (B) Scheme diagram of the two-photon excited Fe-C₃N₄@Ru@HOP (FCRH) nanocomposite for efficient PDT against hypoxic tumor. (C) Fluorescence imaging and micro-CT transillumination fluorescent combination imaging (top right) of FCRH *in vivo*, and its *ex vivo* fluorescence imaging in heart, liver, spleen, lung, kidney and tumor (bottom right). (D) HIF-α, TUNEL, CD31 and H&E staining assays of tumors after various treatments. Reproduced with permission from Ref. [113], Copyright © 2018, Elsevier. Abbreviations: PDT: photodynamic therapy; CT: computed tomography; H&E: hematoxylin and eosin.

NanoPcA caused by amine groups in TEG facilitated highly efficient ROS generation under 655 nm laser irradiation. Therefore, NanoPcA can serve as a PS to hypoxic tumor PDT through type I photoreactions. In addition to the visible light-activated type I PDT mentioned above, NIR-activated type I PDT is also developed for deep tissue penetration depth. Li and co-workers [122] engineered tungsten carbide nanoparticles (W_2C NPs) to produce $\cdot OH$ and 1O_2 via type I and type II reaction mechanisms for NIR-activated dual-type PDT. The synthesized W_2C NPs exhibited strong light absorption in NIR II region and could simultaneously generate $\cdot OH$ and 1O_2 merely under 1064 nm laser irradiation. In addition, the excellent photothermal activity of W_2C NPs allowed synergistic therapeutic effects of PDT/PTT. *In vitro* and *in vivo* tests confirmed the convenient and highly-efficient anti-tumor capability of W_2C NPs

even in hypoxic tumors.

O_2 -economized strategies

Different from the O_2 -replenishing strategies and O_2 -independent strategies mentioned above, O_2 -economized strategies are targeted to regulate tumor hypoxia by decelerating cell respiration. It is noticed that the mitochondria-associated oxidative phosphorylation (OXPHOS) process can lead to excessive physiological O_2 consumption which is well known as cell respiration [123]. Scientists believe that the block of O_2 consumption in OXPHOS by inhibiting the activity of Complex I in the mitochondrial electron transport chain (ETC) would be a feasible and meaningful strategy to relieve tumor hypoxia [124]. In one study, Yang *et al.* [125] synthesized a tailor-made PDT platform (PEG-PCL-IR780-MET NPs) by packaging PSs (IR780)

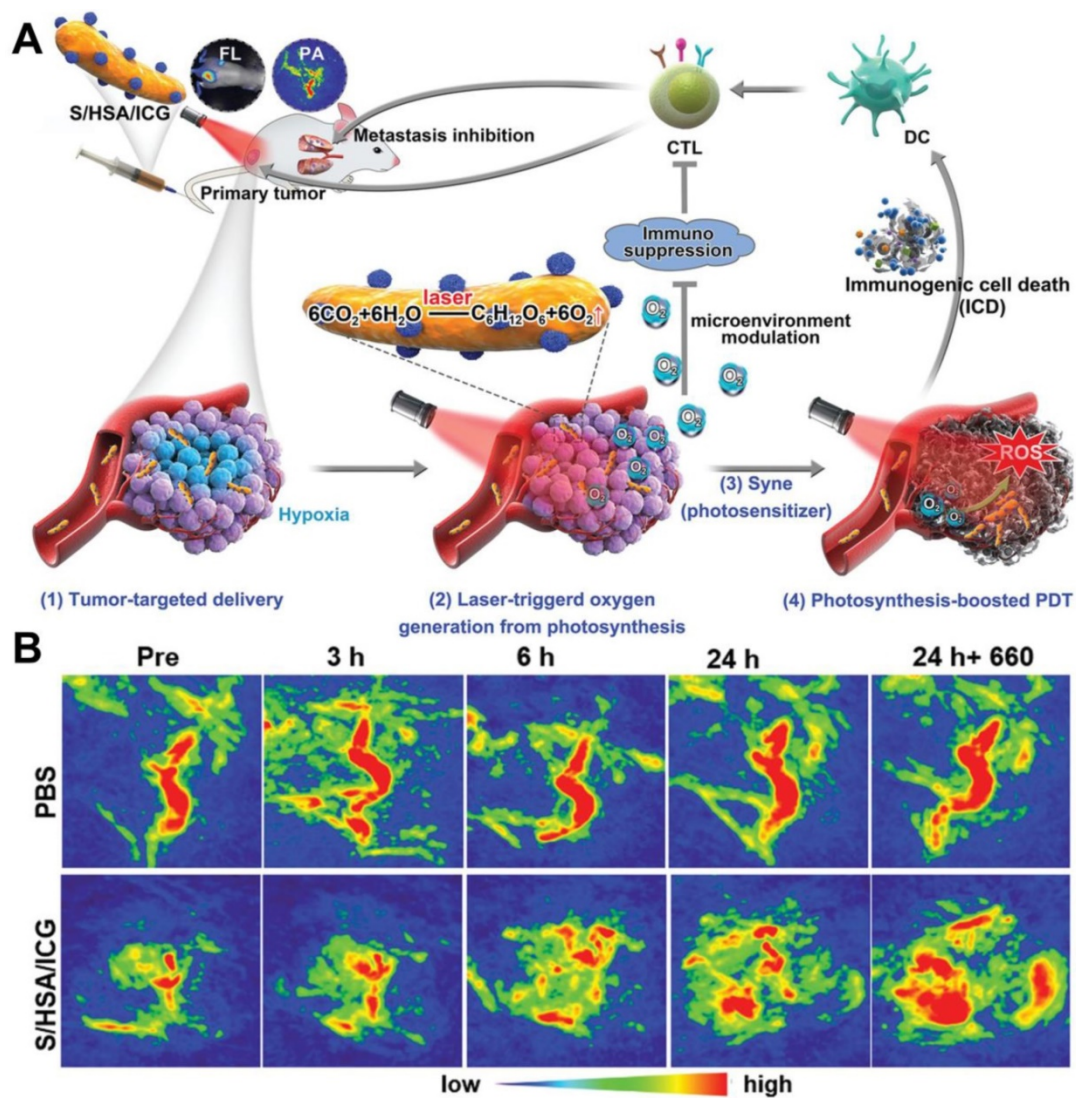


Figure 9. (A) Schematic illustration of S/HSA/ICG as an O_2 generation system for photosynthesis-boosted PDT. (B) PA images of tumors taken at different time points after intravenous injection of PBS and S/HSA/ICG. Reproduced with permission from Ref. [116], Copyright © 2020, Wiley-VCH Verlag GmbH & Co. KGaA, Weinheim. Abbreviations: ICG: indocyanine green; PDT: photodynamic therapy; PA: photoacoustic.

and metformin (MET) in poly (ϵ caprolactone)-poly (ethylene glycol) (PEG-PCL). Once these PEG-PCL-IR780-MET NPs accumulated in tumor tissues, IR780 could generate ROS under 808 nm laser irradiation, and MET could directly inhibit the activity of Complex I in mitochondrial ETC, thus achieving superior PDT efficacy.

In another work, Zhao *et al.* [126] prepared atovaquone (ATO, an oxidative phosphorylation inhibitor) and Ce6-based self-delivery nanomedicine (ACSN) for O₂-economized PDT. With a high drug loading rate, ACSN significantly improved the stability of Ce6 and ATO, and enhanced cell internalization and intratumor permeability as well. The role of ATO in this work is to inhibit the mitochondria respiratory chain, reduce O₂ consumption and relieve hypoxia, thereby increasing the production of ROS and improving the efficiency of PDT (**Figure 11A**). As a result, ACSN exhibited robust inhibition of tumor growth with low systemic toxicity (**Figure 11B-11D**). To further enhance the penetration of drugs into the tumor, Fan *et al.* [127] established sub-50 nm dual-drug nanoparticles (NPs) to encapsulate verteporfin (VER, a kind of PSs) and oxygen-regulator ATO (ATO/VER NPs) to attenuate hypoxia-induced resistance to PDT. In this system, ATO/VER NPs could penetrate into the interior regions of the tumor. Then, the ATO released from

ATO/VER NPs efficiently reduced cellular oxygen consumption by blocking the ETC pathway and further heightened VER to generate ¹O₂. Both *in vitro* and *in vivo* tests proved the powerful anti-tumor PDT effect of ATO/VER NPs.

In addition, Li *et al.* [128] investigated the influence of antiestrogenic drug tamoxifen (TAM) on mitochondria respiration. They successfully devised a ⁻O₂⁻ generator (SORgenTAM) on the basis of TAM. Results of a series of tests confirmed that TAM could disturb the energy metabolism of cells by inhibiting mitochondrial Complex I in ETC. Consequently, TAM significantly overcame the hypoxia resistance in PDT. In addition to MET, ATO and TAM, nitric oxide (NO) also possesses the ability to inhibit cellular respiration and disturb cell metabolism. Yu *et al.* [129] fabricated a PDT-specific O₂ economizer by using poly(D,L-lactide-co-glycolide) nanovesicles (PVs) to co-load NO donor (sodium nitroprusside (SNP)) and tetraphenylporphyrin (TPP). Once the TPP and SNP co-loaded PVs (PV-TS) accumulated in tumors through EPR effect, the released SNP could respond to locally reductive environment and decompose to generate NO that could compete with O₂ by binding to the O₂-binding site of mitochondria for respiration inhibition. As a result, such a PV-TS system showed outstanding antitumor performance toward hypoxic tumors.

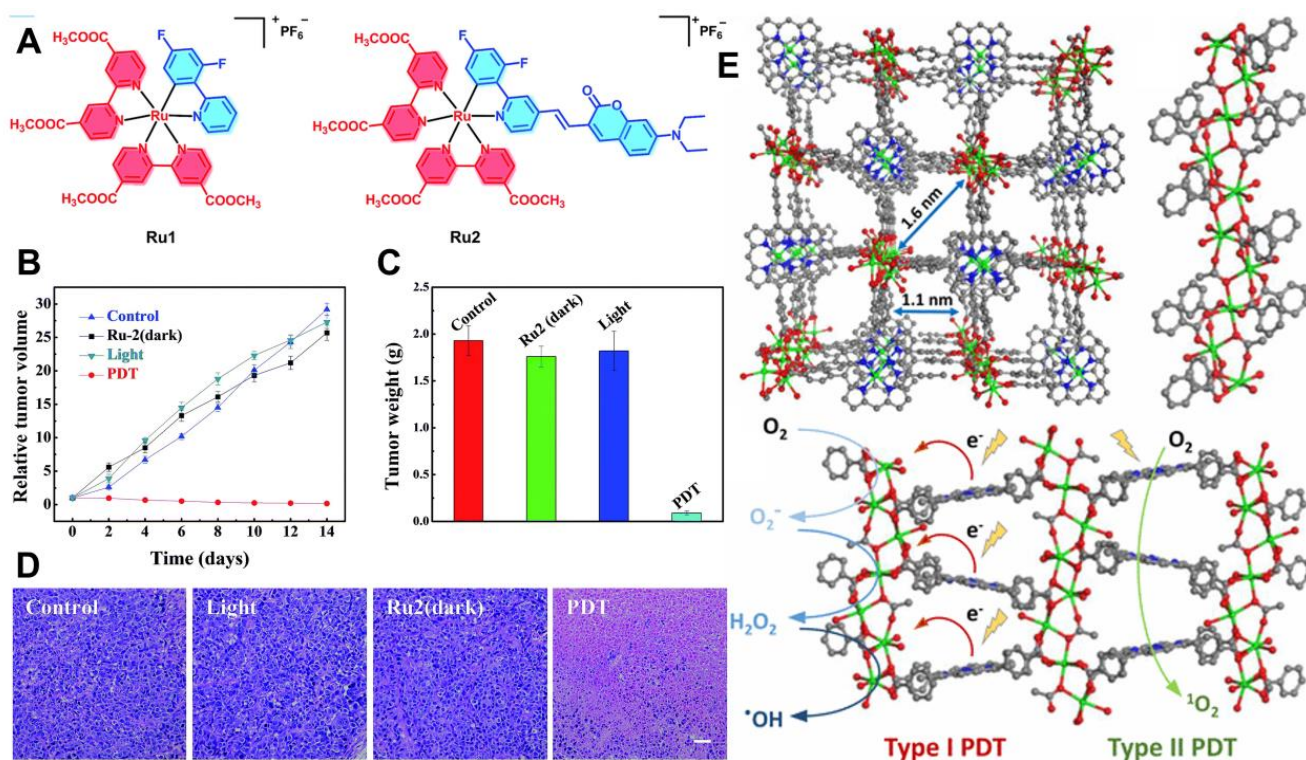


Figure 10. (A) Chemical structures of Ru1 and Ru2. (B) Tumor volume curves of mice after various treatments, and (C) corresponding tumor weights after 14 days of treatment. (D) H&E staining of tumor slices from different groups. Reproduced with permission from Ref. [118], Copyright © 2018, Royal Society of Chemistry. (E) Structure of Ti-TBP and schematic diagram of type I and type II PDT under light irradiation. Reproduced with permission from Ref. [119], Copyright © 2019, American Chemical Society. Abbreviations: H&E: hematoxylin and eosin.

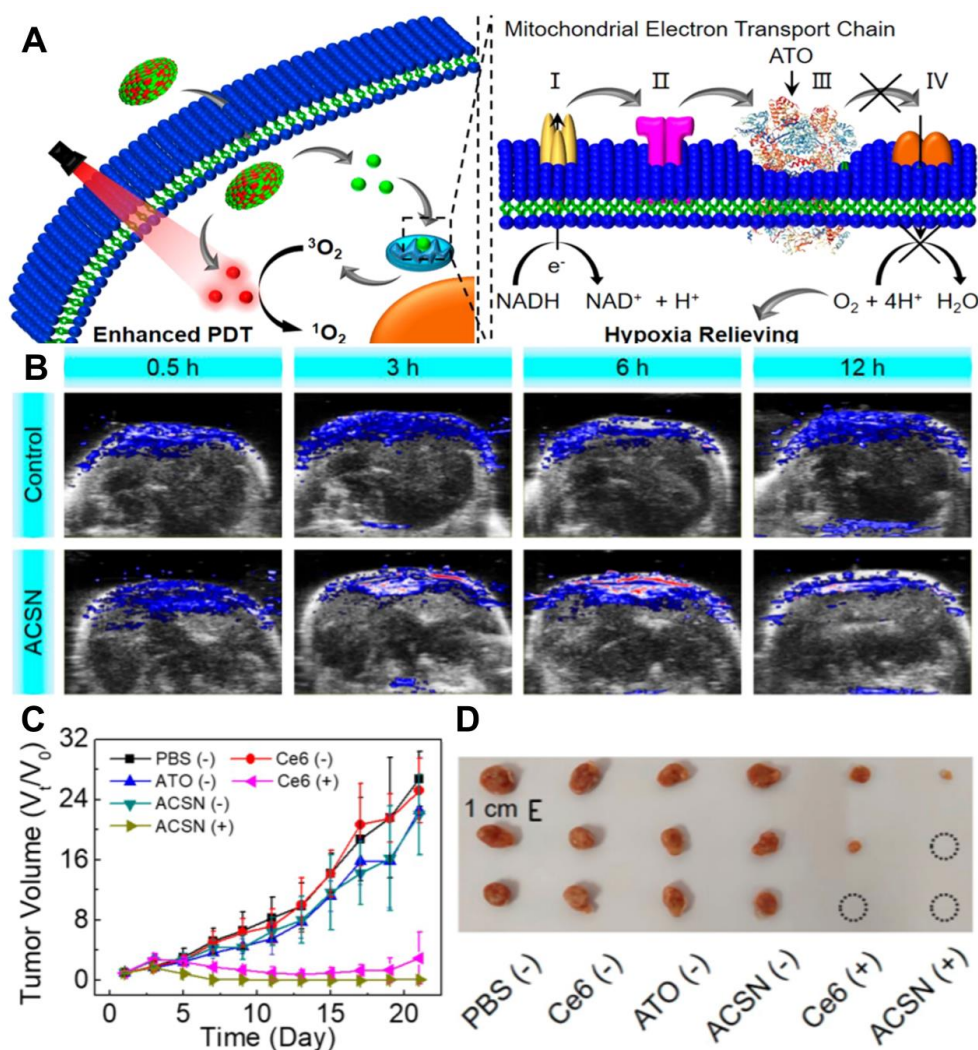


Figure 11. (A) Schematic diagram of mitochondrial respiratory inhibition enhanced PDT against tumor cells. (B) *In vivo* PA images of tumors after various treatments for 0.5, 3, 6, and 12 h. (C) Corresponding tumor volume changes of mice during the 21 days evaluation period with various treatments, and (D) corresponding tumor images at 21st-day post-treatment. Reproduced with permission from Ref. [126]. Copyright © 2020, American Chemical Society. Abbreviations: PDT: photodynamic therapy; PA: photoacoustic.

Summary of innovative strategies for overcoming tumor hypoxia

In this section, different innovative strategies for mitigating the hypoxic tumor microenvironment have been summarized. In general, the number of research publications on hypoxia regulation has grown exponentially. Most of these studies present encouraging results in overcoming tumor hypoxia and ultimately improving cancer therapy. However, we should be cautious about the application of these emerging strategies to circumvent hypoxia, since they are still in the early stage of development and require more rigorous testing before clinical trials.

Topical PDT

In clinical trials to date, PSs are usually administered through intravenous injection, oral or topical delivery. Topical PDT is a non-invasive and rapidly evolving therapeutic form to treat

precancerous cutaneous lesions or non-melanoma skin cancers, such as basal cell carcinoma (BCC), squamous cell carcinoma *in situ*, and actinic keratosis [159]. The topical PS precursors, aminolevulinic acid (ALA) and its derivatives (methyl aminolevulinic acid (MAL) and hexyl aminolevulinic acid (HAL)) are not photosensitive but can be converted endogenously into PpIX by the haem biosynthesis pathway. PpIX that tends to accumulate in malignant cells can be activated by blue or red light to generate ROS, causing selective cellular damage [160]. The advantage of topical PDT is it can treat multiple lesions simultaneously with excellent tolerance and superior cosmetic outcomes.

ALA (a 20% 5-ALA solution in alcohol) is commercially available and FDA approved for the treatment of non-hyperkeratotic actinic keratosis on the face and scalp in combination with blue light (417 nm) [161]. In Europe, a gel formulation of 10% ALA in nano-emulsion was developed and licensed by FDA

to treat actinic keratosis under the excitation of a red light (635 nm) LED lamp [162]. Considering that ALA is a water-soluble amino acid with low lipid solubility and cannot penetrate the stratum corneum, MAL (a 16% MAL topical cream) was used to treat BCC and actinic keratosis in combination with a red light lamp (570–670 nm) [163]. The above three ALA-/MAL-based topical PDT drugs have been tested in clinical studies for several indications. For example, in a phase III trial involving 88 patients with BCCs, ALA PDT showed shorter healing time and better cosmetic outcomes compared to cryosurgery (12-month clinical recurrence rate of 5% versus 13%) [164]. Similarly, a multicenter randomized controlled trial among 196 patients revealed the excellent therapeutic effect of MAL PDT for superficial BCCs (complete response (CR) rate at 3 months: 92.2%, 12-month recurrence rate: 9.3%) [165]. In another phase III comparative trial, 281 patients with BCCs were treated with 10% ALA gel and MAL cream. Effective PDT was observed in both formulations with CRs of >90% [166].

PDT-involved multimodal therapies

Complete eradication of malignant tumors or effective prevention of the metastasis and relapse by PDT alone is difficult due to the inherent defects of PDT. The combination of PDT with other therapies can exploit the advantages of each therapeutic modality to offset the disadvantages of PDT. The interaction between different therapies can not only produce synergistic therapeutic effects, but also improve the anti-tumor efficacy at low-dose PSs or low-power light irradiation, thereby minimizing the potential toxicity to normal tissues. Several combination therapy partners for PDT, such as chemotherapy and immunotherapy, have been approved in initial clinical studies [30]. This section will focus on the research progress of chemo-photodynamic therapy (chemo-PDT) and immuno-photodynamic therapy (immuno-PDT).

Chemo-PDT

The combination of PDT and chemotherapy can induce synergistic therapeutic effects: the PSs can overcome multidrug resistance, while the chemotherapeutic drugs can address the limitations of light penetration and hypoxia-related resistance in PDT and enhance the sensitivity of cancer cells to ROS. Recently, Zhang *et al.* [167] reported an albumin 'nanoglue'-based nanotheranostics for chemo-photodynamic combination therapy, which consists of HSA, chemotherapeutic drug paclitaxel (PTX), and photosensitizer sinoporphyrin sodium (DVDMS). The as-prepared HSA-PTXDVDMS nanoparticles (HPD)

exhibited good stability and effective accumulation in tumors after intravenous injection. Particularly, the HPD showed enhanced antitumor efficacy compared to DVDMS alone, displaying the broad clinical application prospects of chemo-PDT. Similarly, Wang *et al.* [168] constructed an intelligent protoporphyrin-based polymer nanoplatfrom with a multiple stimuli-responsive function for combined chemo-PDT. These polymer micelles (Dex-g-PpIX-g-PBA-SS-CPT (DPPSC)) were composed of dex-tran (Dex), PpIX, anticancer drug camptothecin (CPT), and pH-sensitive linker. Once the micelles enter the tumor, the photochemical internalization (PCI) effect of PpIX could facilitate cellular uptake, and the CPT could be released from the micelles by the hydrolysis of pH-sensitive linker to achieve chemotherapy. The combined chemo-PDT is expected to maximize the therapeutic effect and minimize the side effects of chemotherapeutic agent.

Preclinical and clinical studies have shown that PDT combined with chemotherapy is an effective tumor treatment option [175]. For example, Hong *et al.* [176] compared the long-term curative effect of PDT alone (porfimer sodium) and PDT combined with chemotherapy (gemcitabine or gemcitabine with cisplatin) on patients with cholangiocarcinoma. There was no statistically significant difference in tumor node metastasis (TNM) stage, bismuth type, CA 19-9 level, and pre-PDT albumin level between two groups. However, PDT with chemotherapy resulted in significant improvement of overall survival compared to PDT alone (median survival: 538 days versus 334 days). It was easily concluded that PDT combined with chemotherapy for advanced hilar cholangiocarcinoma is superior to PDT alone. Especially, PDT-mediated vascular permeabilization can enhance the accumulation of drugs in tumors for enhanced efficacy [177]. Luo *et al.* [178] used a semi-mechanistic pharmacokinetic-pharmacodynamic (PK/PD) model to investigate the effect of PDT on drug delivery. Long-circulating liposomes loaded with doxorubicin (DOX) and porphyrin-phospholipid (PoP) PSs were administered intravenously to mice. Tumor irradiation with 665 nm laser light (200 J/cm²) for 1 h showed increased drug accumulation, as evidenced by an overall 7-fold increase in DOX area under the tumor curve in the PK/PD model. This study adequately demonstrated the enhancement of PDT-based drug delivery.

Immuno-PDT

The occurrence and metastasis of tumors is highly related to the evasion of immune surveillance system. Various studies have profoundly demonstrated that PDT can cause immunogenic cell

death (ICD) to release damage-associated molecules and consequently improve the immunogenicity of tumors [169]. Moreover, the combination of PDT with checkpoint-blockade immunotherapy can better eliminate primary tumors, inhibit metastasis, and prevent recurrence [179]. For example, Xu *et al.* [180] synthesized UCNPs to simultaneously load Ce6 and imiquimod (R837, a Toll-like-receptor-7 agonist) for immuno-PDT. In tumor experiments, UCNP-Ce6-R837 could control the regrowth of primary tumors under NIR irradiation, while its effect on distant tumors was limited. Anti-CTLA-4 alone decreased tumor growth rate, but did not lead to the regression of primary or distant tumors. UCNP-Ce6-R837 combined with CTLA-4 blockade not only displayed excellent efficacy in eliminating primary tumor but also resulted in strong antitumor immunities to inhibit the growth of distant tumors. Similarly, Zhang *et al.* [170] fabricated an immunoadjuvant nano-agent (γ -PGA@GOx@Mn,Cu-CDs) by integrating γ -glutamic acid (γ -PGA), glucose oxidase (GOx) and Mn,Cu-doped carbon dots (CDs) with excellent photodynamic effect under 730 nm laser irradiation. After combined with PD-L1 antibody for checkpoint-blockade immunotherapy, γ -PGA@GOx@Mn,Cu-CDs significantly ablated primary tumors and suppressed distant tumors through antitumor immune response. In another work, Sun *et al.* [171] successfully developed a sorafenib and Ce6 co-loaded ROS-responsive nanoparticle (NP-sfb/ce6) for combined immuno-PDT. Under 660 nm laser irradiation, the Ce6-produced ROS destroyed the nanoparticles, leading to the boosted cascade release of sorafenib. The low-dose PDT and rapidly released sorafenib synergistically inhibited tumor growth by inducing T cell-dependent antitumor immune responses and reprogramming the immunosuppressive TME. Thus, the combination of PDT with immunotherapy has the potential to eradicate tumors and trigger immune memory to prevent tumor recurrence.

Conclusions and future perspectives

PDT has made dramatic progress over the past few decades because of its feasibility and effectiveness in cancer treatment. Recent advances in nanotechnology have opened promising avenues for developing new PDT systems and provided multifaceted opportunities to circumvent the intrinsic drawbacks in current PDT paradigms. This review has systematically summarized and discussed the latest research development of PDT in light source, PSs, and tumor hypoxia. For light source, we have highlighted the latest innovative strategies based on NIR light, X-ray and internal light. In terms of PSs, we have introduced different types of PSs and the

research progress of nanocarriers and targeting conjugates for improving the stability and targeting ability of PSs. As for tumor hypoxia, we have summarized three kinds of innovative strategies to overcome the hypoxic limitation in PDT. Nevertheless, in spite of all the remarkable progress, there still exist some issues in PDT as detailed below.

(i) As described above, a critical challenge for PDT in cancer therapy is the limited penetration depth of light. Visible light is not an ideal choice due to the strong light absorption of tissue. NIR light is limited by the penetration depth of less than 2 cm. Moreover, the energy of NIR light may not be high enough to effectively activate PSs to generate adequate ROS. X-ray can deeply penetrate into tissues, but it exhibits low ROS generation efficiency and can cause side effects on healthy tissues. This technique needs to be improved to achieve better therapeutic effect with low doses of X-ray radiation. Although internal light is not affected by the light delivery efficiency, its photoexcitation efficiency is unsatisfactory. Therefore, an ideal light source is still under exploration.

Recently, researchers have started to utilize microwaves [130], radio-waves [131], ultrasound [132], EF [133], MF [134], and electromagnetic fields (EMF) [135] to induce PDT. Microwave irradiation can cause local hyperthermia and lead to tumor sensitization, which is useful for increasing the blood supply to the tumor and promoting ROS generation. Ultrasound, a type of mechanical wave, can penetrate into cancer targets buried deep in human tissues. It can precisely focus on specific tumor sites and effectively activate the cytotoxicity of PSs, ultimately triggering tumor cell destruction with minimal damage to adjacent normal tissues [172]. The electroporation effect caused by EF can help PSs pass through the cell membrane, thus enhancing the PDT effect. MF can promote the accumulation of magnetic PSs in tumorous region. Hence, future research is encouraged to study more about the above excitation modes. Additionally, light radiation conditions such as exposure time and pulse frequency should be taken into consideration.

(ii) The therapeutic effect of PDT is largely related to the choice of PSs that are expected to possess strong tumor targeting ability, excellent stability, and high ROS generation efficiency. Since the morphology, particle size, and surface modification can significantly affect the stability and targeting efficiency of PSs, a lot of efforts are needed to develop ideal PSs that can be activated by long wavelengths with high ROS yields. The application of nanomaterial agents in PDT can overcome some shortcomings of conventional PSs. The combination of

PSs and magnetic nano-emulsion may be a new strategy to realize targeted MF-induced PDT. Moreover, transition metal complexes can also be a choice to construct PSs with tumor-targeting ability and high ROS generation efficiency. For example, some tris-chelated Ir^{III} complexes exhibit long-lived triplet excited states and phosphorescence, which allows them to generate destructive ¹O₂ efficiently even under hypoxic conditions [136]. In addition, it is also very important to choose the appropriate concentration and administration mode of PSs.

(iii) As mentioned earlier, tumor hypoxia can significantly hamper the antitumor effect of PDT. Although many innovative strategies including O₂-replenishing, O₂-independent, and O₂-economized strategies have been put forward to deal with this issue, there are still several issues need to be concerned: 1) how to quantify the O₂ supply level of O₂-replenishing strategies for PDT; 2) how to obtain biocompatible hypoxia-confronted PDT systems without obvious toxicity; 3) how to transform the innovative PDT agents for hypoxic tumor elimination into clinical applications. In addition, great efforts can also be made to develop other new strategies. For instance, the recently emerged strategies to improve blood flow, reduce ROS scavenging, remodel extracellular matrix, and combine with hypoxia-activated therapeutic modalities have also become effective approaches to overcome tumor hypoxia [137-139].

In spite of the aforementioned challenges, underlying mechanism issues (e.g. pharmacokinetic/pharmacodynamic analysis) are also crucial in determining the optimal conditions for PDT and ensuring the long-term biosafety of PDT agents. Moreover, it is worth noting that the currently used tumor models are simplified. They are rather different from the actual situation. In addition, for the multifunctional theranostic nanomaterials currently proposed for PDT, a comprehensive understanding of the way they behave as a collective entity and affect complex biological systems is still lagging behind. Admittedly, none of these nanomaterials has been approved by FDA for clinical application. Therefore, it is urgent to conduct in-depth characterization of them to check whether they will interfere with each other's functions and impede the overall therapeutic effect. In this regard, standardized physicochemical characterization and evaluation protocols must be established to achieve the regulatory review of nanotechnology-based PDT agents. Undoubtedly, there is still a long way to go before PDT become a first-line treatment option for cancer. It is hoped that this review would advance future development of PDT and provide encouraging possibilities for

effective cancer therapy.

Abbreviations

PDT: photodynamic therapy; PSs: photosensitizers; ROS: reactive oxygen species; ¹O₂: singlet oxygen; O₂⁻: superoxide radicals; OH: hydroxyl radicals; ¹PS*: excited singlet state; ³PS*: triplet state; O₂: oxygen; NIR: near-infrared; MOFs: metal-organic frameworks; UCNPs: upconversion nanoparticles; GQD: graphene quantum dot; IPA: isophthalic acid; RTP: room-temperature phosphorescence; LDHs: layered double hydroxides; RB: rose bengal; AIE: aggregation-induced emission; Hb: hemoglobin; CPNs: conjugated polymer nanoparticles; CRET: chemiluminescence resonance energy transfer; PLM-hydrogel: PersLum material hydrogel; HpD: hematoporphyrin derivative; DhE: dihaematoporphyrin ether; FDA: Food and Drug Administration; ZnPc: zinc phthalocyanine; Ce6: chlorin e6; MB: methylene blue; BP: black phosphorus; TiO₂: titanium dioxide; TMOs: transition metal oxides; g-C₃N₄: graphitic-phase carbon nitride; PCM: phase change materials; sMnO₂: ultrasmall manganese dioxide; PA: photoacoustic; NPs: nanoparticles; Exos: exosomes; PMA: amphiphilic polymer; CM: cancer cell membrane; M-MONs: magnetic mesoporous organosilica nanoparticles; PpIX: protoporphyrin IX; TMDs: transition metal dichalcogenides; TEG: triethylene glycol; HA: hyaluronic acid; PFCs: perfluorocarbons; RBCs: artificial red blood cells; UiO-66: zirconium (IV)-based MOFs; TME: tumor microenvironment; Ca: calcium; Au: gold; Pt: platinum; Mn: manganese; Cu: copper; CD: cyclodextrin; PDA: polydopamine; RuFc: Ruthenium (II) complex; Cyan: *Synechococcus elongatus* PCC 7942; Syne: *Synechococcus* 7942; TBP: 5,10,15,20-tetra (p-benzoato) porphyrin; W₂C NPs: tungsten carbide nanoparticles; OXPHOS: mitochondria-associated oxidative phosphorylation; ETC: electron transport chain; MET: metformin; ATO: atovaquone; VER: verteporfin; TAM: tamoxifen; NO: nitric oxide; PVs: poly(D,L-lactide-co-glycolide) nanovesicles; SNP: sodium nitroprusside; TPP: tetraphenylporphyrin; EF: electrical fields; MF: magnetic fields; EMF: electromagnetic fields.

Acknowledgements

This work was supported by the National Natural Science Foundation of China (NSFC: 21521005, 21971007, 21671013) and the Fundamental Research Funds for the Central Universities (XK1802-6, XK1803-05).

Contributions

Min Wei and Ruizheng Liang conceived the review topic. Tingting Hu wrote the manuscript in consultation with all the other authors. Zhengdi Wang and Weicheng Shen arranged all the figures. Min Wei, Ruizheng Liang and Dan Yan modified the manuscript. All authors contributed to the final manuscript.

Competing Interests

The authors have declared that no competing interest exists.

References

- Lin H, Chen Y, Shi J. Nanoparticle-triggered *in situ* catalytic chemical reactions for tumour-specific therapy. *Chem Soc Rev*. 2018; 47: 1938-1958.
- Bray F, Ferlay J, Soerjomataram I, Siegel RL, Torre LA, Jemal A. Global cancer statistics 2018: GLOBOCAN estimates of incidence and mortality worldwide for 36 cancers in 185 countries. *CA-Cancer J Clin*. 2018; 68: 394-424.
- Wan SS, Zeng JY, Cheng H, Zhang XZ. ROS-induced NO generation for gas therapy and sensitizing photodynamic therapy of tumor. *Biomaterials*. 2018; 185: 51-62.
- Manghnani PN, Wu W, Xu S, Hu F, Teh C, Liu B. Visualizing photodynamic therapy in transgenic zebrafish using organic nanoparticles with aggregation-induced emission. *Nano-Micro Lett*. 2018; 10: 61-69.
- Dougherty TJ, Gomer CJ, Henderson BW, Jori G, Kessel D, Korbelik M, et al. Photodynamic therapy. *J Natl Cancer Inst*. 1998; 90: 889-905.
- Staicu A, Pascu A, Nuta A, Sorescu A, Raditoiu V, Pascu ML. Studies about phthalocyanine photosensitizers to be used in photodynamic therapy. *Rom Rep Phys*. 2013; 65: 1032-1051.
- Li X, Zheng BD, Peng XH, Li SZ, Ying JW, Zhao Y, et al. Phthalocyanines as medicinal photosensitizers: developments in the last five years. *Coord Chem Rev*. 2019; 379: 147-160.
- Yang Z, Wang J, Ai S, Sun J, Mai X, Guan W. Self-generating oxygen enhanced mitochondrion-targeted photodynamic therapy for tumor treatment with hypoxia scavenging. *Theranostics*. 2019; 9: 6809-23.
- Ding H, Yu H, Dong Y, Tian R, Huang G, Boothman DA, et al. Photoactivation switch from type II to type I reactions by electron-rich micelles for improved photodynamic therapy of cancer cells under hypoxia. *J Controlled Release*. 2011; 156: 276-280.
- Zhang C, Zhao K, Bu W, Ni D, Liu Y, Feng J, et al. Marriage of scintillator and semiconductor for synchronous radiotherapy and deep photodynamic therapy with diminished oxygen dependence. *Angew Chem Int Ed*. 2015; 54: 1770-1774.
- Xu X, Huang B, Zeng Z, Chen J, Huang Z, Guan Z, et al. Broaden sources and reduce expenditure: tumor-specific transformable oxidative stress nanoamplifier enabling economized photodynamic therapy for reinforced oxidation therapy. *Theranostics*. 2020; 10: 10513-10530.
- Zhu T, Shi L, Yu C, Dong Y, Qiu F, Shen L, et al. Ferroptosis promotes photodynamic therapy: supramolecular photosensitizer-inducer nanodrug for enhanced cancer treatment. *theranostics*. 2019; 9: 3293-307.
- Master A, Livingston M, Gupta AS. Photodynamic nanomedicine in the treatment of solid tumors: perspectives and challenges. *J Controlled Release*. 2013; 168: 88-102.
- Lin T, Zhao X, Zhao S, Yu H, Cao W, Chen W, et al. O₂-generating MnO₂ nanoparticles for enhanced photodynamic therapy of bladder cancer by ameliorating hypoxia. *Theranostics*. 2018; 8: 990-1004.
- Succo G, Rosso S, Fadda GL, Fantini M, Crossetti E. Salvage photodynamic therapy for recurrent nasopharyngeal carcinoma. *Photodiagn Photodyn Ther*. 2014; 11: 63-70.
- Yang M, Yang T, Mao C. Enhancement of photodynamic cancer therapy by physical and chemical factors. *Angew Chem Int Ed*. 2019; 58: 14066-14080.
- Fan W, Huang P, Chen X. Overcoming the Achilles' heel of photodynamic therapy. *Chem Soc Rev*. 2016; 45: 6488-6519.
- Li X, Zhang Q, Ahmad Z, Huang J, Ren Z, Weng W, et al. Near-infrared luminescent CaTiO₃:Nd³⁺ nanofibers with tunable and trackable drug release kinetics. *J Mater Chem B*. 2015; 3: 7449-7456.
- Liu H, Fu Y, Li Y, Ren Z, Li X, Han G, et al. A fibrous localized drug delivery platform with NIR-triggered and optically monitored drug release. *Langmuir*. 2016; 32: 9083-9090.
- Zhou Z, Song J, Nie L, Chen X. Reactive oxygen species generating systems meeting challenges of photodynamic cancer therapy. *Chem Soc Rev*. 2016; 45: 6597-6626.
- Huang RB, Mocherla S, Heslinga MJ, Charoenphol P, Eniola-Adefeso O. Dynamic and cellular interactions of nanoparticles in vascular-targeted drug delivery. *Mol Membr Biol*. 2010; 27: 312-327.
- Kruijt B, van der Snoek EM, Sterenborg HJ, Amelink A, Robinson DJ. A dedicated applicator for light delivery and monitoring of PDT of intra-anal intraepithelial neoplasia. *Photodiagn Photodyn Ther*. 2010; 7: 3-9.
- Etcheverry ME, Pasquale MA, Garavaglia M. Photodynamic therapy of HeLa cell cultures by using LED or laser sources. *J Photochem Photobiol B*. 2016; 160: 271-277.
- Panjehpour M, Overholt BF, Haydek JM. Light sources and delivery devices for photodynamic therapy in the gastrointestinal tract. *Gastrointest Endosc Clin N Am*. 2000; 10: 513-532.
- Jeon YM, Lee HS, Jeong D, Oh HK, Ra KH, Lee MY. Antimicrobial photodynamic therapy using chlorin e6 with halogen light for acne bacteria-induced inflammation. *Life Sci*. 2015; 124: 56-63.
- Moslemi N, Soleiman-zadeh Azar P, Bahador A, Rouzmeh N, Chiniforush N, Paknejad M, et al. Inactivation of aggregatibacter actinomycetemcomitans by two different modalities of photodynamic therapy using toluidine blue O or radachlorin as photosensitizers: an *in vitro* study. *Lasers Med Sci*. 2015; 30: 89-94.
- Reddy ML, Bejoymohandas KS. Evolution of 2, 3'-bipyridine class of cyclometalating ligands as efficient phosphorescent iridium (III) emitters for applications in organic light emitting diodes. *J Photochem Photobiol C*. 2016; 29: 29-47.
- Turan IS, Yildiz D, Turksoy A, Gunaydin G, Akkaya EU. A bifunctional photosensitizer for enhanced fractional photodynamic therapy: singlet oxygen generation in the presence and absence of light. *Angew Chem Int Ed*. 2016; 55: 2875-2878.
- Lan M, Zhao S, Liu W, Lee C, Zhang W, Wang P. Photosensitizers for photodynamic therapy. *Adv Healthc Mater*. 2019; 8: 1900132.
- Li X, Lovell JF, Yoon J, Chen X. Clinical development and potential of photothermal and photodynamic therapies for cancer. *Nat Rev Clin Oncol*. 2020; 17: 657-674.
- Liu C, Liu B, Zhao J, Di Z, Chen D, Gu Z, et al. Nd³⁺-sensitized upconversion metal-organic frameworks for mitochondria-targeted amplified photodynamic therapy. *Angew Chem Int Ed*. 2020; 59: 1-6.
- Zhang D, Wen L, Huang R, Wang H, Hu X, Xing D. Mitochondrial specific photodynamic therapy by rare-earth nanoparticles mediated near-infrared graphene quantum dots. *Biomaterials*. 2018; 153: 14-26.
- Gao R, Mei X, Yan D, Liang R, Wei M. Nano-photosensitizer based on layered double hydroxide and isophthalic acid for singlet oxygenation and photodynamic therapy. *Nat Commun*. 2018; 9: 2798.
- Sun W, Luo L, Feng Y, Cai Y, Zhuang Y, Xie RJ, et al. Aggregation-induced emission gold clustoluminogens for enhanced low-dose X-ray-induced photodynamic therapy. *Angew Chem Int Ed*. 2019; 58: 1-8.
- Zhong X, Wang X, Zhan G, Tang Y, Yao Y, Dong Z, et al. NaCeF₄:Gd,Tb scintillator as an X-ray responsive photosensitizer for multimodal imaging-guided synchronous radio/radiodiagnostic therapy. *Nano Lett*. 2019; 19: 8234-8244.
- Jiang L, Bai H, Liu L, Lv F, Ren X, Wang S. Luminescent, oxygen-supplying, hemoglobin-linked conjugated polymer nanoparticles for photodynamic therapy. *Angew Chem*. 2019; 131: 10770-10775.
- Sun SK, Wu J, Wang H, Zhou L, Zhang C, Cheng R, et al. Turning solid into gel for high-efficient persistent luminescence-sensitized photodynamic therapy. *Biomaterials*. 2019; 218: 119328.
- Stacey OJ, Pope SJ. Supramolecular functionalized polybenzoxazines from azobenzene carboxylic acid/azobenzene pyridine complexes: synthesis, surface properties, and specific interactions. *RSC Adv*. 2013; 3: 25550-25564.
- Zhao HJ, Li L, Zheng CX, Hao YW, Niu MY, Hu YJ, et al. An intelligent dual stimuli-responsive photosensitizer delivery system with O₂-supplying for efficient photodynamic therapy. *Colloids Surf B*. 2018; 167: 299-309.
- Chen WH, Luo GF, Qiu WX, Lei Q, Liu LH, Wang SB, et al. Mesoporous silica-based versatile theranostic nanopatform constructed by layer-by-layer assembly for excellent photodynamic/chemo therapy. *Biomaterials*. 2017; 117: 54-65.
- Schwartz S, Absolon K, Bull HV. Some relationships of porphyrins, X-rays and tumors. *Univ Minn Med Bull*. 1955; 27: 7-8.
- Triesscheijn M, Baas P, Schellens JH, Stewart FA. Photodynamic therapy in oncology. *Oncol*. 2006; 11: 1034-1044.
- Bellnier DA, Greco WR, Loewen GM, Nava H, Oseroff AR, Dougherty TJ. Clinical pharmacokinetics of the PDT photosensitizers porfimer sodium (photofrin), 2-[1-Hexyloxyethyl]-2-devinyl pyropheophorbide-a (photoclor) and 5-ALA-induced protoporphyrin IX. *Laser Surg Med*. 2006; 38: 439-444.
- Sharman WM, Allen CM, van Lier JE. Photodynamic therapeutics: basic principles and clinical applications. *Drug Discov Today*. 1999; 4: 507-517.
- Li X, Lee S, Yoon J. Supramolecular photosensitizers rejuvenate photodynamic therapy. *Chem Soc Rev*. 2018; 47: 1174-1188.
- Zhang J, Jiang C, Figueiró Longo JP, Azevedo RB, Zhang H, Muehlmann LA. An updated overview on the development of new photosensitizers for anticancer photodynamic therapy. *Acta Pharm Sin B*. 2018; 8: 137-146.
- Moraes M, Vasconcelos RC, Longo JP, Muehlmann LA, Azevedo RB, Lemos TM, et al. Effects of photodynamic therapy mediated by nanoemulsion containing chloro-aluminum phthalocyanine: a histologic and immunohistochemical study in human gingiva. *Photodiagn Photodyn Ther*. 2015; 12: 592-597.
- Yue C, Zhang C, Alfranca G, Yang Y, Jiang X, Yang Y, et al. Near-infrared light triggered ROS-activated theranostic platform based on C6-CPT-UCNPs for

- simultaneous fluorescence imaging and chemo-photodynamic combined therapy. *Theranostics*. 2016; 6: 456-469.
49. Garg AD, Krysko DV, Vandenabeele P, Agostinis P. Hypericin-based photodynamic therapy induces surface exposure of damage-associated molecular patterns like HSP70 and calreticulin. *Cancer Immunol Immunother*. 2012; 61: 215-221.
50. Graciano TB, Coutinho TS, Cressoni CB, Freitas CP, Pierre MB, Pereira SA, *et al*. Using chitosan gels as a toluidine blue O delivery system for photodynamic therapy of buccal cancer: *in vitro* and *in vivo* studies. *Photodiagnosis Photodyn Ther*. 2015; 12: 98-107.
51. Delaey E, Laar F, Vos D, Kamuhabwa A, Jacobs P, Witte P. A comparative study of the photosensitizing characteristics of some cyanine dyes. *J Photochem Photobiol B Biol*. 2000; 55: 27-36.
52. Ren XD, Hao XY, Li HC, Ke MR, Zheng BY, Huang JD. Progress in the development of nanosensitizers for X-ray-induced photodynamic therapy. *Drug Discov Today*. 2018; 23: 1791.
53. Panzarini E, Inguscio V, Fimia GM, Dini L. Rose bengal acetate photodynamic therapy (RBAC-PDT) induces exposure and release of damage-associated molecular patterns (DAMPs) in human HeLa cells. *PLoS One*. 2014; 9: e105778.
54. Vogel E, Köcher M, Schmickler H, Lex J. Porphycene-a novel porphyrin isomer. *Angew Chem Int Ed*. 1986; 25: 257-259.
55. Kataoka H, Nishie H, Hayashi N, Tanaka M, Nomoto A, Yano S, *et al*. New photodynamic therapy with next-generation photosensitizers. *Ann Transl Med*. 2017; 5: 183.
56. Vijayaraghavan P, Liu CH, Vankayala R, Chiang CS, Hwang KC. Designing multi-branched gold nanochains for NIR light activated dual modal photodynamic and photothermal therapy in the second biological window. *Adv Mater*. 2014; 26: 6689-6695.
57. Sharma A, Goyal AK, Rath G. Recent advances in metal nanoparticles in cancer therapy. *J Drug Target*. 2018; 26: 617-632.
58. Chaix A, Rajoua K, Stojanovic V, Cheikh KE, Bouffard E, Brocéro A, *et al*. Two-photon fluorescence imaging and therapy of cancer cells with anisotropic gold-nanoparticle-supported porous silicon nanostructures. *Chem Nano Mat*. 2018; 4: 343-347.
59. Shi L, Hernandez B, Selke M. Singlet oxygen generation from water-soluble quantum dot-organic dye nanocomposites. *J Am Chem Soc*. 2006; 128: 6278-6279.
60. Ge J, Lan M, Zhou B, Liu W, Guo L, Wang H, *et al*. A graphene quantum dot photodynamic therapy agent with high singlet oxygen generation. *Nat Commun*. 2014; 5: 4596.
61. Wang H, Yang X, Shao W, Chen S, Xie J, Zhang X, *et al*. Ultrathin black phosphorus nanosheets for efficient singlet oxygen generation. *J Am Chem Soc*. 2015; 137: 11376-11382.
62. Zhang C, Chen WH, Liu LH, Qiu WX, Yu WY, Zhang XZ. An O₂ self-supplementing and reactive-oxygen-species-circulating amplified nanoplatfrom via H₂O/H₂O₂ splitting for tumor imaging and photodynamic therapy. *Adv Funct Mater*. 2017; 27: 1700626.
63. Pan C, Ou M, Cheng Q, Zhou Y, Yu Y, Li Z, *et al*. Z-Scheme heterojunction functionalized pyrite nanosheets for modulating tumor microenvironment and strengthening pphoto/chemodynamic therapeutic effects. *Adv Funct Mater*. 2020; 30: 1906466.
64. Liu G, Zou J, Tang Q, Yang X, Zhang Y, Zhang Q, *et al*. Surface modified Ti₃C₂ MXene nanosheets for tumor targeting photothermal/photodynamic/chemo synergistic therapy. *ACS Appl Mater Interfaces*. 2017; 9: 40077-40086.
65. Lin LS, Cong ZX, Li J, Ke KM, Guo SS, Yang HH, *et al*. Graphitic phase C₃N₄ nanosheets as efficient photosensitizers and pH-responsive drug nanocarriers for cancer imaging and therapy. *J Mater Chem B*. 2014; 2: 1031-1037.
66. Zhang S, Li Q, Yang N, Shi Y, Ge W, Wang W, *et al*. Phase-change materials based nanoparticles for controlled hypoxia modulation and enhanced phototherapy. *Adv Funct Mater*. 2019; 29: 1906805.
67. Lai RC, Yeo RW, Tan KH, Lim SK. Exosomes for drug delivery-a novel application for the mesenchymal stem cell. *Biotechnol Adv*. 2013; 31: 543-551.
68. Fang RH, Kroll AV, Gao W, Zhang L. Cell membrane coating nanotechnology. *Adv Mater*. 2018; 30: 1706759.
69. Pan S, Pei L, Zhang A, Zhang Y, Zhang C, Huang M, *et al*. Passion fruit-like exosome-PMA/Au-BSA/Ce6 nanovehicles for real-time fluorescence imaging and enhanced targeted photodynamic therapy with deep penetration and superior retention behavior in tumor. *Biomaterials*. 2020; 230: 119606.
70. Wang Z, Zhang F, Shao D, Chang Z, Wang L, Hu H, *et al*. Janus nanobullets combine photodynamic therapy and magnetic hyperthermia to potentiate synergistic anti-metastatic immunotherapy. *Adv Sci*. 2019; 6: 1901690.
71. Cheng H, Fan G, Fan J, Yuan P, Deng F, Qiu X, *et al*. Epigenetics-inspired photosensitizer modification for plasma membrane-targeted photodynamic tumor therapy. *Biomaterials*. 2019; 224: 119497.
72. Bechet D, Auger F, Couleaud P, Marty E, Ravasi L, Durieux N, *et al*. Multifunctional ultrasmall nanoplatforms for vascular-targeted interstitial photodynamic therapy of brain tumors guided by real-time MRI. *Nanomedicine*. 2015; 11: 657-670.
73. Cao B, Yang M, Zhu Y, Qu X, Mao C. Stem cells loaded with nanoparticles as a drug carrier for *in vivo* breast cancer therapy. *Adv Mater*. 2014; 26: 4627-4631.
74. Li W, Peng J, Tan L, Wu J, Shi K, Qu Y, *et al*. Mild photothermal therapy/photodynamic therapy/chemotherapy of breast cancer by Lyp-1 modified Docetaxel/IR820 Co-loaded micelles. *Biomaterials*. 2016; 106: 119-133.
75. Shibu ES, Hamada M, Murase N, Biju V. Nanomaterials formulations for photothermal and photodynamic therapy of cancer. *J Photochem Photobiol C*. 2013; 15: 53-72.
76. Sah U, Sharma K, Chaudhri N, Sankar M, Gopinath P. Antimicrobial photodynamic therapy: single-walled carbon nanotube (SWCNT)-porphyrin conjugate for visible light mediated inactivation of staphylococcus aureus. *Colloids Surf B*. 2018; 162: 108-117.
77. Benachour H, Seve A, Bastogne T, Frochot C, Vanderesse R, Jasniowski J, *et al*. Multifunctional peptide-conjugated hybrid silica nanoparticles for photodynamic therapy and MRI. *Theranostics*. 2012; 2: 889-904.
78. Sunderland K, Yang M, Mao C. Phage-enabled nanomedicine: from probes to therapeutics in precision medicine. *Angew Chem Int Ed*. 2017; 56: 1964-1992.
79. Meng HM, Zhao D, Li N, Chang JB. A graphene quantum dot-based multifunctional two-photon nanoprobe for the detection and imaging of intracellular glutathione and enhanced photodynamic therapy. *Analyst*. 2018; 143: 4967-4973.
80. Gao S, Zheng P, Li Z, Feng X, Yan W, Chen S, *et al*. Biomimetic O₂-evolving metal-organic framework nanoplatform for highly efficient photodynamic therapy against hypoxic tumor. *Biomaterials*. 2018; 178: 83-94.
81. Liang J, Zheng Y, Wu X, Tan C, Ji L, Mao Z. A tailored multifunctional anticancer nanodelivery system for ruthenium-based photosensitizers: tumor microenvironment adaption and remodeling. *Adv Sci*. 2020; 7: 1901992.
82. Wang S, Chen Z, Gao F, Zhang C, Zou M, Ye J, *et al*. Remodeling extracellular matrix based on functional covalent organic framework to enhance tumor photodynamic therapy. *Biomaterials*. 2020; 234: 119772.
83. Liang R, Tian R, Ma L, Zhang L, Hu Y, Wang J, *et al*. A supermolecular photosensitizer with excellent anticancer performance in photodynamic therapy. *Adv Funct Mater*. 2014; 24: 3144-3151.
84. Lan G, Ni K, Xu Z, Veroneau SS, Song Y, Lin W. Nanoscale metal-organic framework overcomes hypoxia for photodynamic therapy primed cancer immunotherapy. *J Am Chem Soc*. 2018; 140: 5670-5673.
85. Liu T, Wang C, Cui W, Gong H, Liang C, Shi X, *et al*. Combined photothermal and photodynamic therapy delivered by PEGylated MoS₂ nanosheets. *Nanoscale*. 2014; 6: 11219-11225.
86. Fan W, Bu W, Shen B, He Q, Cui Z, Liu Y, *et al*. Intelligent MnO₂ nanosheets anchored with upconversion nanoprob for concurrent pH-/H₂O₂-responsive UCL imaging and oxygen-elevated synergetic therapy. *Adv Mater*. 2015; 27: 4155-4161.
87. Huang K, Li Z, Lin J, Han G, Huang P. Two-dimensional transition metal carbides and nitrides (MXenes) for biomedical applications. *Chem Soc Rev*. 2018; 47: 5109-5124.
88. Hilgenbrink AR, Low PS. Folate receptor-mediated drug targeting: from therapeutics to diagnostics. *J Pharmacol Sci*. 2005; 94: 2135-2146.
89. Bourré L, Giuntini F, Eggleston IM, Wilson M, MacRobert AJ. 5-Aminolaevulinic acid peptide prodrugs enhance photosensitization for photodynamic therapy. *Mol Canc Therapeut*. 2008; 7: 1720-1729.
90. Sibirian-Vazquez M, Jensen TJ, Vicente MG. Porphyrin-retinamides: synthesis and cellular studies. *Bioconjugate Chem*. 2007; 18: 1185-1193.
91. Sol V, Chaleix V, Champavier Y, Granet R, Huang YM, Krausz P. Glycosyl bisporphyrin conjugates: synthesis and potential application in PDT. *Bioorg Med Chem*. 2006; 14: 7745-7760.
92. Schmidt-Erfurth U, Diddens H, Birngruber R, Hasan T. Photodynamic targeting of human retinoblastoma cells using covalent low-density lipoprotein conjugates. *Br J Canc*. 1997; 75: 54-61.
93. Bolfarini GC, Siqueira-Moura MP, Demets GF, Morais PC, Tedesco AC. *In vitro* evaluation of combined hyperthermia and photodynamic effects using magnetoliposomes loaded with cucurbituril zinc phthalocyanine complex on melanoma. *J Photochem Photobiol B Biol*. 2012; 115: 1-4.
94. Savellano MD, Hasan T. Photochemical targeting of epidermal growth factor receptor: a mechanistic study. *Clin Canc Res*. 2005; 11: 1658-1668.
95. Savellano MD, Pogue BW, Hoopes PJ, Vitetta ES, Paulsen KD. Multi-epitope HER2 targeting enhances photoimmunotherapy of HER2-overexpressing cancer cells with pyropheophorbide-a immunconjugates. *Canc Res*. 2005; 65: 6371-6379.
96. Yang L, Wang J, Yang S, Lu Q, Li P, Li N. Rod-shape MSN@MoS₂ nanoplatform for FL/MSOT/CT imaging-guided photothermal and photodynamic therapy. *Theranostics*. 2019; 9: 3992-4005.
97. Ma Z, Zhang M, Jia X, Bai J, Ruan Y, Wang C, *et al*. Fe III-doped two-dimensional C₃N₄ nanofusiform: a new O₂-evolving and mitochondriatargeting photodynamic agent for MRI and enhanced antitumor therapy. *Small*. 2016; 12: 5477-5487.
98. Sahu A, Kwon I, Tae G. Improving cancer therapy through the nanomaterials-assisted alleviation of hypoxia. *Biomaterials*. 2020; 228: 119578.
99. Duan L, Yan X, Wang A, Jia Y, Li J. Highly loaded hemoglobin spheres as promising artificial oxygen carriers. *ACS Nano*. 2012; 6: 6897-6904.
100. Luo Z, Zheng M, Zhao P, Chen Z, Siu F, Gong P, *et al*. Self-monitoring artificial red cells with sufficient oxygen supply for enhanced photodynamic therapy. *Sci Rep*. 2016; 6: 23393.
101. Wang S, Yuan F, Chen K, Chen G, Tu K, Wang H, *et al*. Synthesis of hemoglobin conjugated polymeric micelle: A ZnPc carrier with oxygen self-compensating ability for photodynamic therapy. *Biomacromolecules*. 2015; 16: 2693-2700.
102. Wang J, Liu L, You Q, Song Y, Sun Q, Wang Y, *et al*. All-in-one theranostic nanoplatform based on hollow MoS_x for photothermally-manuevered oxygen self-enriched photodynamic therapy. *Theranostics*. 2018; 8: 955-971.

103. Cheng Y, Cheng H, Jiang C, Qiu X, Wang K, Huan W, *et al.* Perfluorocarbon nanoparticles enhance reactive oxygen levels and tumour growth inhibition in photodynamic therapy. *Nat Commun.* 2015; 6: 8785.
104. Zhou HC, Long JR, Yaghi OM. Introduction to metal-organic frameworks. *Chem Rev.* 2012; 112: 673-674.
105. Cai X, Xie Z, Ding B, Shao S, Liang S, Pang M, *et al.* Monodispersed copper(I)-based nano metal-organic framework as a biodegradable drug carrier with enhanced photodynamic therapy efficacy. *Adv Sci.* 2019; 6: 1900848.
106. Yang N, Xiao W, Song X, Wang W, Dong X. Recent advances in tumor microenvironment hydrogen peroxide-responsive materials for cancer photodynamic therapy. *Nano-Micro Lett.* 2020; 12: 15.
107. Zheng DW, Li B, Li CX, Fan JX, Lei Q, Li C, *et al.* Carbon-dot-decorated carbon nitride nanoparticles for enhanced photodynamic therapy against hypoxic tumor via water splitting. *ACS Nano.* 2016; 10: 8715-8722.
108. Hu H, Qian X, Chen Y. Microalgae-enabled photosynthetic alleviation of tumor hypoxia for enhanced nanotherapies. *Sci Bull.* in press. doi: 10.1016/j.scib.2020.07.019.
109. Chen H, Tian J, He W, Guo Z. H₂O₂-activatable and O₂-evolving nanoparticles for highly efficient and selective photodynamic therapy against hypoxic tumor cells. *J Am Chem Soc.* 2015; 137: 1539-1547.
110. Chen Q, Feng L, Liu J, Zhu W, Dong Z, Wu Y, *et al.* Intelligent albumin-MnO₂ nanoparticles as pH-/H₂O₂-responsive dissociable nanocarriers to modulate tumor hypoxia for effective combination therapy. *Adv Mater.* 2016; 28: 7129-7136.
111. Yao C, Wang W, Wang P, Zhao M, Li X, Zhang F. Near-infrared upconversion mesoporous cerium oxide hollow biophotocatalyst for concurrent pH-/H₂O₂-responsive O₂-evolving synergetic cancer therapy. *Adv Mater.* 2018; 30: 1704833.
112. Singh S. Cerium oxide based nanozymes: redox phenomenon at biointerfaces. *Biointerphases.* 2016; 11: 04B202.
113. Li RQ, Zhang C, Xie BR, Yu WY, Qiu WX, Cheng H, *et al.* A two-photon excited O₂-evolving nanocomposite for efficient photodynamic therapy against hypoxic tumor. *Biomaterials.* 2019; 194: 84-93.
114. Cohen JE, Goldstone AB, Paulsen MJ, Shudo Y, Steele AN, Edwards BB, *et al.* An innovative biologic system for photon-powered myocardium in the ischemic heart. *Sci Adv.* 2017; 3: e1603078.
115. Huo M, Wang L, Zhang L, Wei C, Chen Y, Shi J. Photosynthetic tumor oxygenation by photosensitizer-containing cyanobacteria for enhanced photodynamic therapy. *Angew Chem.* 2019; 131: 2-10.
116. Liu L, He H, Luo Z, Zhou H, Liang R, Pan H, *et al.* *In situ* photocatalyzed oxygen generation with photosynthetic bacteria to enable robust immunogenic photodynamic therapy in triple-negative breast cancer. *Adv Funct Mater.* 2020; 30: 1910176.
117. Gilson RC, Black KC, Lane D, Achilefu S. Hybrid TiO₂-ruthenium nanophotosensitizer synergistically produces reactive oxygen species in both hypoxic and normoxic conditions. *Angew Chem Int Ed.* 2017; 56: 10717.
118. Lv Z, Wei H, Li Q, Su X, Liu S, Zhang KY, *et al.* Achieving efficient photodynamic therapy under both normoxia and hypoxia using cyclometalated Ru(II) photosensitizer through type I photochemical process. *Chem Sci.* 2018; 9: 502-512.
119. Lan G, Ni K, Veroneau SS, Feng X, Nash GT, Luo T, *et al.* Titanium-based nanoscale metal-organic framework for Type I photodynamic therapy. *J Am Chem Soc.* 2019; 141: 4204-4208.
120. Bevernaegie R, Doix B, Bastien E, Diman A, Decottignies A, Feron O, *et al.* Exploring the phototoxicity of hypoxic active iridium(III)-based sensitizers in 3D tumor spheroids. *J Am Chem Soc.* 2019; 141: 18486-18491.
121. Li X, Lee D, Huang JD, Yoon J. Phthalocyanine-assembled nanodots as photosensitizers for highly efficient Type I photoreactions in photodynamic therapy. *Angew Chem Int Ed.* 2018; 57: 9885-9890.
122. Li S, Yang W, Liu Y, Song XR, Liu R, Chen G, *et al.* Engineering of tungsten carbide nanoparticles for imaging-guided single 1,064 nm laser-activated dual-type photodynamic and photothermal therapy of cancer. *Nano Res.* 2018; 11: 4859-4873.
123. Xia DL, Xu PP, Luo XY, Zhu JF, Gu HY, Huo D, *et al.* Overcoming hypoxia by multistage nanoparticle delivery system to inhibit mitochondrial respiration for photodynamic therapy. *Adv Funct Mater.* 2019; 29: 1807294.
124. Molina JR, Sun Y, Protopopova M, Gera S, Bandi M, Bristow C, *et al.* An inhibitor of oxidative phosphorylation exploits cancer vulnerability. *Nat Med.* 2018; 24: 1036-1046.
125. Yang Z, Wang J, Liu S, Li X, Miao L, Yang B, *et al.* Defeating relapsed and refractory malignancies through a nano-enabled mitochondria-mediated respiratory inhibition and damage pathway. *Biomaterials.* 2020; 229: 119580.
126. Zhao L, Zheng R, Chen H, Liu L, Zhao X, Liu H, *et al.* Self-delivery nanomedicine for O₂-economized photodynamic tumor therapy. *Nano Lett.* 2020; 20: 2062-2071.
127. Fan Y, Zhou T, Cui P, He Y, Chang X, Xing L, *et al.* Modulation of intracellular oxygen pressure by dual-drug nanoparticles to enhance photodynamic therapy. *Adv Funct Mater.* 2019; 29: 1806708.
128. Li M, Shao Y, Kim J, Pu Z, Zhao X, Huang H, *et al.* Unimolecular photodynamic O₂-economizer to overcome hypoxia resistance in phototherapeutics. *J Am Chem Soc.* 2020; 142: 5380-5388.
129. Yu W, Liu T, Zhang M, Wang Z, Ye J, Li C, *et al.* O₂ economizer for inhibiting cell respiration to combat the hypoxia obstacle in tumor treatments. *ACS Nano.* 2019; 13: 1784-1794.
130. Yao M, Ma L, Li L, Zhang J, Lim R, Chen W, *et al.* A new modality for cancer treatment-nanoparticle mediated microwave induced photodynamic therapy. *J Biomed Nanotechnol.* 2016; 12: 1835-1851.
131. Manthe RL, Foy SP, Krishnamurthy N, Sharma B, Labhasetwar V. Tumor ablation and nanotechnology. *Mol Pharm.* 2010; 7: 1880-1898.
132. Wang P, Li C, Wang X, Xiong W, Feng X, Liu Q, *et al.* Anti-metastatic and pro-apoptotic effects elicited by combination photodynamic therapy with sonodynamic therapy on breast cancer both *in vitro* and *in vivo*. *Ultrason Sonochem.* 2015; 23: 116-127.
133. Kulbacka J, Kotulska M, Rembalkowska N, Choromska A, Kaminska I, Garbicz A, *et al.* Cellular stress induced by photodynamic reaction with CoTPPS and MnTMPyPCs in combination with electroporation in human colon adenocarcinoma cell lines (LoVo and LoVoDX). *Cell Stress Chaperones.* 2013; 18: 719-731.
134. Park S, Hwang J, Kwon Y, Cheon C. Antenna system applicable to microwave non-invasive hyperthermia lipolysis. *Electron Lett.* 2012; 48: 1179-1181.
135. Radeva M, Berg A, Berg H. Induction of apoptosis and necrosis in cancer cells by electric fields, electromagnetic fields, and photodynamically active quinoids. *Electromagn Biol Med.* 2004; 23: 185-200.
136. Zhang P, Chiu CK, Huang H, Lam YP, Habtemariam A, Malcomson T, *et al.* Organoiridium photosensitizers induce specific oxidative attack on proteins within cancer cells. *Angew Chem Int Ed.* 2017; 56: 14898-14902.
137. Feng L, Tao D, Dong Z, Chen Q, Chao Y, Liu Z, *et al.* Near-infrared light activation of quenched liposomal Ce6 for synergistic cancer phototherapy with effective skin protection. *Biomaterials.* 2017; 127: 13-24.
138. Huang F, Xia F. A smart photodynamic therapy strategy: depletion of glutathione in cancer cells. *Sci Bull.* 2017; 62: 312-313.
139. Li L, Yang Z, Fan W, He L, Cui C, Zou J, *et al.* *In situ* polymerized hollow mesoporous organosilica biocatalysis nanoreactor for enhancing ROS-mediated anticancer therapy. *Adv Funct Mater.* 2019; 30: 1907716.
140. Jeong H, Huh M, Lee SJ, Koo H, Kwon IC, Jeong SY, *et al.* Photosensitizer-conjugated human serum albumin nanoparticles for effective photodynamic therapy. *Theranostics.* 2011; 1: 230-239.
141. Dong Y, Yang J, Liu H, Wang T, Tang S, Zhang J, *et al.* Site-specific drug-releasing polypeptide nanocarriers based on dual-pH response for enhanced therapeutic efficacy against drug-resistant tumors. *Theranostics.* 2015; 5: 890-904.
142. Lo PC, Morgade MS, Pandey RK, Ng DK, Torres T, Dumoulin F. The unique features and promises of phthalocyanines as advanced photosensitizers for photodynamic therapy of cancer. *Chem Soc Rev.* 2020; 49: 1041-1056.
143. Shafirstein G, Bellnier D, Oakley E, Hamilton S, Potasek M, Beeson K, *et al.* Interstitial photodynamic therapy-a focused review. *Cancers.* 2017; 9: 12.
144. Liu J, Shi J, Nie W, Wang S, Liu G, Cai K. Recent progress in the development of multifunctional nanoplatfor for precise tumor phototherapy. *Adv Healthc Mater.* 2020; 2001207.
145. Lucky SS, Soo KC, Zhang Y. Nanoparticles in photodynamic therapy. *Chem Rev.* 2015; 115: 1990-2042.
146. Yang W, Read PW, Mi J, Baisden JM, Reardon KA, Lerner JM, *et al.* Semiconductor nanoparticles as energy mediators for photosensitizer-enhanced radiotherapy. *Int J Radiat Oncol.* 2018; 72: 633-635.
147. Rossi F, Bedogni E, Bigi F, Rimoldi T, Cristofolini L, Pinelli S, *et al.* Porphyrin conjugated SiC/SiO_x nanowires for X-ray-excited photodynamic therapy. *Sci Rep.* 2015; 5: 7606.
148. Shafirstein G, Bellnier DA, Oakley E, Hamilton S, Habitzruther M, Tworek L, *et al.* Irradiance controls photodynamic efficacy and tissue heating in experimental tumours: implication for interstitial PDT of locally advanced cancer. *Brit J Cancer.* 2018; 119: 1191-1199.
149. Ismael FS, Amasha H, Bachir W. Optimized cylindrical diffuser powers for interstitial PDT breast cancer treatment planning: a simulation study. *BioMed Res Int.* in press. doi: 10.1155/2020/2061509.
150. Vermandel M, Quidet M, Vignion-Dewalle AS, Leroy HA, Leroux B, Mordon S, *et al.* Comparison of different treatment schemes in 5-ALA interstitial photodynamic therapy for high-grade glioma in a preclinical model: an MRI study. *Photodiagn Photodyn.* 2019; 25: 166-176.
151. Kwiatkowski S, Knap B, Przystupski D, Saczko J, Kędzierska E, Knap-Czop K, *et al.* Photodynamic therapy-mechanisms, photosensitizers and combinations. *Biomed Pharmacother.* 2018; 106: 1098-1107.
152. Kou J, Dou D, Yang L. Porphyrin photosensitizers in photodynamic therapy and its applications. *Oncotarget.* 2017; 8: 81591-81603.
153. Sun P, Wang G, Hou H, Yuan P, Deng W, Wang C, *et al.* A water-soluble phosphorescent conjugated polymer brush for tumor-targeted photodynamic therapy. *Polym Chem.* 2017; 8: 5836.
154. Zhou Z, Liu J, Rees T, Wang H, Li X, Chao H, *et al.* Heterometallic Ru-Pt metallacycle for two-photon photodynamic therapy. *P Natl Acad Sci USA.* 2018; 115: 5664-5669.
155. Jiao L, Song L, Cui J, Peng X. A near-infrared heptamethine aminocyanine dye with a long-lived excited triplet state for photodynamic therapy. *Chem Commun.* 2018; 54: 9198.
156. Shi H, Sun W, Wang Q, Gu G, Si W, Huang W, *et al.* A thienyl-substituted diketopyrrolopyrrole derivative with efficient reactive oxygen species generation for photodynamic therapy. *ChemPlusChem.* 2016; 81: 515-520.
157. Zheng Z, Zhang T, Liu H, Chen Y, Kwok R, Ma C, *et al.* Bright near-infrared aggregation-induced emission luminogens with strong two-photon absorption, excellent organelle specificity, and efficient photodynamic therapy. *ACS Nano.* 2018; 12: 8145-8159.

158. Zhang Y, Bo S, Feng T, Qin X, Wan Y, Jiang S, *et al.* A versatile theranostic nanoemulsion for architecture dependent multimodal imaging and dually augmented photodynamic therapy. *Adv Mater.* 2019; 31: 1806444.
159. Morton CA, Szeimies RM, Sidoroff A, Braathen LR. European guidelines for topical photodynamic therapy part 1: treatment delivery and current indications-actinic keratoses, Bowen's disease, basal cell carcinoma. *J Eur Acad Dermatol Venereol.* 2013; 27: 536-544.
160. Kim M, Jung HY, Park HJ. Topical PDT in the treatment of benign skin diseases: principles and new applications. *Int J Mol Sci.* 2015; 16: 23259-23278.
161. Barr H, Kendall C, Reyes-Goddard J, Stone N. Clinical aspects of photodynamic therapy. *Sci Prog.* 2002; 85: 131-150.
162. Lu YG, Wu JJ, He Y, Yang HZ, Yang YD. Efficacy of topical aminolevulinic acid photodynamic therapy for the treatment of verruca plana. *Photomed Laser Surg.* 2010; 28: 561-563.
163. Gaullier JM, Berg K, Peng Q, Anholt H, Selbo PK, Ma LW, *et al.* Use of 5-aminolevulinic acid esters to improve photodynamic therapy on cells in culture. *Cancer Res.* 1997; 57: 1481-1486.
164. Wang I, Bendsoe N, Klinteberg CA, Enejder AM, Svanberg K. Photodynamic therapy vs. cryosurgery of basal cell carcinomas: results of a phase III clinical trial. *Br J Dermatol.* 2001; 144: 832-840.
165. Szeimies RM, Ibbotson S, Murrell DF, Rubel D, Frambach Y, Berker D, *et al.* A clinical study comparing methyl aminolevulinate photodynamic therapy and surgery in small superficial basal cell carcinoma (8–20 mm), with a 12-month follow-up. *J Eur Acad Dermatol Venereol.* 2008; 22: 1302-1311.
166. Morton CA, Dominicus R, Radny P, Dirschka T, Hauschild A, Reinhold U, *et al.* A randomized, multinational, noninferiority, phase III trial to evaluate the safety and efficacy of BF-200 aminolaevulinic acid gel vs. methyl aminolaevulinate cream in the treatment of nonaggressive basal cell carcinoma with photodynamic therapy. *Br J Dermatol.* 2018; 179: 309-319.
167. Zhang Y, Wan Y, Chen Y, Blum NT, Lin J, Huang P. Ultrasound-enhanced chemo-photodynamic combination therapy by using albumin "nanoglue"-based nanotheranostics. *ACS Nano.* 2020; 14: 5560-5569.
168. Wang Y, Wei G, Zhang X, Xu F, Xiong X, Zhou S. A step-by-step multiple stimuli-responsive nanoplatform for enhancing combined chemo-photodynamic therapy. *Adv Mater.* 2017; 29: 1605357.
169. Ng CW, Li J, Pu K. Recent progresses in phototherapy-synergized cancer immunotherapy. *Adv Funct Mater.* 2018; 28: 1804688.
170. Zhang M, Wang W, Wu F, Zheng T, Ashley J, Mohammadniaei M, *et al.* Biodegradable poly(γ -glutamic acid)@glucose oxidase@carbon dot nanoparticles for simultaneous multimodal imaging and synergetic cancer therapy. *Biomaterials.* 2020; 252: 120106.
171. Sun X, Cao Z, Mao K, Wu C, Chen H, Wang J, *et al.* Photodynamic therapy produces enhanced efficacy of antitumor immunotherapy by simultaneously inducing intratumoral release of sorafenib. *Biomaterials.* 2020; 240: 119845.
172. Chen H, Zhou X, Gao Y, Zheng B, Tang F, Huang J. Recent progress in development of new sonosensitizers for sonodynamic cancer therapy. *Drug Discov Today.* 2014; 19: 502.
173. Yong Y, Zhou L, Gu Z, Yan L, Tian G, Zheng X, *et al.* WS₂ nanosheet as a new photosensitizer carrier for combined photodynamic and photothermal therapy of cancer cells. *Nanoscale.* 2014; 6: 10394-10403.
174. Chen J, Fan T, Xie Z, Zeng Q, Xue P, Zheng T, *et al.* Advances in nanomaterials for photodynamic therapy applications: status and challenges. *Biomaterials.* 2020; 237: 119827.
175. Luo D, Carter KA, Miranda D, Lovell JF. Chemophototherapy: an emerging treatment option for solid tumors. *Adv Sci.* 2017; 4: 1600106.
176. Hong MJ, Cheon YK, Lee EJ, Lee TY, Shim CS. Long-term outcome of photodynamic therapy with systemic chemotherapy compared to photodynamic therapy alone in patients with advanced hilar cholangiocarcinoma. *Gut Liver.* 2014; 8: 318-323.
177. Snyder JW, Greco WR, Bellnier DA, Vaughan L, Henderson BW. Photodynamic therapy: a means to enhanced drug delivery to tumors. *Cancer Res.* 2003; 63: 8126-8131.
178. Luo D, Carter KA, Molins EA, Straubinger NL, Geng J, Shao S, *et al.* Pharmacokinetics and pharmacodynamics of liposomal chemophototherapy with short drug-light intervals. *J Control Release.* 2019; 297: 39-47.
179. Cramer GM, Moon EK, Cengel KA, Busch TM. Photodynamic therapy and immune checkpoint blockade. *Photochem Photobiol.* in press. doi: 10.1111/php.13300.
180. Xu J, Xu L, Wang C, Yang R, Zhuang Q, Han X, *et al.* Near-infrared-triggered photodynamic therapy with multitasking upconversion nanoparticles in combination with checkpoint blockade for immunotherapy of colorectal cancer. *ACS Nano.* 2017; 11: 4463-4474.